LEVEL II

12

B5

Report NAVTRAEQUIPCEN 80-C-0055-1

AN OPTIMAL CONTROL MODEL ANALYSIS OF DATA FROM A SIMULATED HOVER TASK

Sheldon Baron
Bolt Beranek and Newman Inc.
10 Moulton Street
Cambridge, Massachusetts 02238

May 1981

FINAL REPORT JUNE 1980 - FEBRUARY 1981

DoD DISTRIBUTION STATEMENT

Approved for public release; distribution unlimited.

NAVAL TRAINING EQUIPMENT CENTER
ORLANDO, FLORIDA 32813

Report NAVTRAEQUIPCEN 80-C-0055-1

Unclassified

SECURITY CLASSIFICATION OF THIS PAGE (When Data Entered)

REPORT DOCUMENTATION PAGE	READ INSTRUCTIONS BEFORE COMPLETING FORM
1. REPORT NUMBER (18) NAVTRAEQUIPCEN 80-C-0055-1 (19)	2. GOVT ACCESSION NO. AD-A099 895
4. TITLE (and Subtitle) (6) AN OPTIMAL CONTROL MODEL ANALYSIS OF DATA FROM A SIMULATED HOVER TASK.	5. TYPE OF REPORT & PERIOD COVERED (9) Final Report, June 1980 - February 1981
	6. PERFORMING ORG. REPORT NUMBER
7. AUTHOR(s) (10) Sheldon Baron	8. CONTRACT OR GRANT NUMBER(s) (15) N61339-80-C-0055
9. PERFORMING ORGANIZATION NAME AND ADDRESS Bolt Beranek and Newman Inc. 10 Moulton Street Cambridge, MA 02238	10. PROGRAM ELEMENT, PROJECT, TASK AREA & WORK UNIT NUMBERS 0785 (12) 64
11. CONTROLLING OFFICE NAME AND ADDRESS (11)	12. REPORT DATE May 1981
	13. NUMBER OF PAGES 54
14. MONITORING AGENCY NAME & ADDRESS(if different from Controlling Office)	15. SECURITY CLASS. (of this report) Unclassified
	15a. DECLASSIFICATION/DOWNGRADING SCHEDULE

16. DISTRIBUTION STATEMENT (of this Report)

17. DISTRIBUTION STATEMENT (of the abstract entered in Block 20, if different from Report)

18. SUPPLEMENTARY NOTES

19. KEY WORDS (Continue on reverse side if necessary and identify by block number)

Simulation Modelling	Visual Display Delay
Optimal Control Model	Motion Platform
Helicopter Hover	G-Seat
Motion Cueing	Flight Simulation

20. ABSTRACT (Continue on reverse side if necessary and identify by block number)

This report describes application of the Optimal Control Model for pilot vehicle analysis to a simulated helicopter hover task. The model is used to predict the effects on performance of changes in motion cues, visual delay and movement of the hover reference point (ship movement). The predicted results are compared with data obtained in a separate experimental study of these effects. The OCM correctly predicts almost all the trends

DD 1 JAN 1473 EDITION OF 1 NOV 65 IS OBSOLETE

060100 ACH

Unclassified

SECURITY CLASSIFICATION OF THIS PAGE (When Data Entered)

observed in the data and its predictions are all within the bounds of pilot-to-pilot variability.

FOREWORD

Mathematic models are used to summarize data from a variety of experiments and to predict outcomes which can then be tested. In flight simulation, various aspects of the closed-loop, pilot/vehicle control system have been modelled: techniques of control modelling and system identification are used to develop aerodynamic models for simulations; pilots' regulatory behavior is well described; and work is underway to define (in a manner consistent with engineering analysis) the perceptual and information processing capabilities of human controllers.

In the work reported herein, the system acted upon by the Bolt, Beranek and Newman, Inc. Optimal Control Model was extended to represent helicopter hover and the closed-loop control of helicopter pilots hovering a marginally stable vehicle was fitted. The results modelled were collected in support of the specification development of the LAMPS MK III trainer, and the present work was to extend the cueing representable by control models to that provided by motion platforms and g-seats. Details of the simuation equipment used--the drive rules for the motion platform, g-seat, and visual display--are contained in NAVTRAEQUIPCEN IH-321.

G. L. Ricard

G. L. RICARD
Scientific Officer

PREFACE

The analytic study reported herein is in support of and complements an empirical study conducted jointly by the Naval Training Equipment Center and NASA-Langley Research Center. The author wishes to thank Russell Parrish, Roland Bowles and Burnell McKissick of NASA for their essential help in providing an appropriate vehicle model and the empirical data needed for the study.

TABLE OF CONTENTS

LIST OF ILLUSTRATIONS

LIST OF TABLES

SECTION I
INTRODUCTION

The development of engineering requirements for man-in-the-loop simulation is a complex task involving numerous trade-offs between simulation fidelity and costs, accuracy and speed, etc. The principal issues confronting the developer of a simulation involve the design of the cue (motion and visual) environment so as to meet simulation objectives, and the design of the digital simulation model to fulfill the real-time requirements with adequate accuracy.

In specifying the cue environment the designer must establish the need for particular cues as well as the requisite fidelity for their presentation. The choices made here are important because the validity and utility of the resulting simulation can be critically dependent upon them and because the decisions involve major costs of the simulation. Unfortunately, these decisions are quite difficult to arrive at rationally, inasmuch as the choices depend on complex psychological as well as engineering factors. The requirements will be governed by the purpose of the simulation; training simulators have different needs than research simulators. They will also be problem dependent (e.g., the need for motion cues in the analysis of aircraft control in a gusty environment will depend on the gust response of the aircraft). Finally, the capabilities of the adaptive human controller both help and compound the problem. The human pilot may be able to compensate for simulator shortcomings and maintain system performance, however, this could result in negative transfer in a training environment or reduced acceptability of the device or an incorrect evaluation in a research simulation.

The design of the simulation model has become increasingly important and difficult as digital computers play a more central role in the simulations. The need for an adequate discrete simulation is also related closely to the cue generation problem inasmuch as the errors and, in particular, the delays introduced by the simulation will be present in the information cues utilized by the pilot.

"Past experience," open loop measurements, and subjective feedback from pilots are all helpful in developing the engineering requirements for simulators. However, for simulations in which the operator's principal task is flight control, it would be very useful to have analytic models for the pilot/vehicle (simulator) system. Such models would have several potential uses. They could be used to examine quantitatively, in a closed-loop context, the (inevitable) trade-offs in simulator design prior to commitment to prototype or full scale development. The design of elements or algorithms to compensate for simulator shortcomings would be facilitated by modelling of this type. The models can serve as insightful ways of looking at and compressing empirical data so that it can be extrapolated to

new situations. Finally, the parameters of an analytic model may prove to be sensitive measures of operator performance and adaptation.

The potential value of analytic models in the simulator design and evaluation process has been recognized in recent years and several development efforts have been undertaken. Of particular relevance to the work described here are several recent studies involving application of the Optimal Control Model (OCM) for pilot/vehicle analysis. Baron, Muralidharan and Kleinman[1] developed techniques for using the OCM to predict the effects on performance of certain simulation model design parameters, such as integration scheme, sample rate, data hold device, etc. The model was applied to a relatively simple air-to-air tracking task and showed significant sensitivity to several parameters. Model results were later compared (Baron and Muralidharan)[2] with data from an experimental study of Ashworth, McKissick and Parrish[3] and the agreement was very encouraging.

In another study,[4] the OCM was used to examine the closed-loop consequences in a helicopter hover task of the performance limitations associated with a computer generated image visual system and a six-degree of freedom motion system. The hover task was linearized and decoupled into separate longitudinal and lateral control tasks. Performance/workload effects of these simulation elements were analyzed by incorporating elaborated sensory perception sub-models in the OCM. The model results suggested that simulator deficiencies of a reasonable nature (by current standards) could result in substantial performance and/or workload infidelity with respect to the task in flight. Unfortunately, there were no corresponding experimental data to confirm or deny these predictions.

1 Baron, S., Muralidharan, R., and Kleinman, D.L., "Closed Loop Models for Analyzing Engineering Requirements for Simulators," NASA CR-2965, Feb. 1980.

2 Baron, S. and Muralidharan, R., "The Analysis of Flight Control Simulator Characteristics Using a Closed-Loop Pilot Vehicle Model," BBN Rept. No. 4329, Feb. 1980.

3 Ashworth, B.R., McKissick, B.T., and Parrish, R.V., "The Effects of Simulation Fidelity on Air-to-Air Tracking," Proc. of Fifteenth Annual Conference on Manual Control, Wright State University, Dayton, OH, March 1979.

4 Baron, S., Lancraft, R., and Zacharias, G., "Pilot/Vehicle Model Analysis of Visual and Motion Cue Requirements in Flight Simulation," NASA CR-3212, Oct. 1980.

Finally, we mention the brief study of Baron[5] to integrate the earlier efforts into a Multi-Cue OCM and to apply the resulting model to analyze effects of control loader dynamics and a g-seat cue on the air-to-air tracking problem investigated earlier.[6] The results of this study have been partially validated empirically but further definition of the proprioceptive model appears necessary.* The Multi-Cue model described by Baron[7] provides the analytic basis for the current investigation.

This report describes work performed under Contract N61339-80-C-0055 for the Naval Training Equipment Center. The effort involved application of the Multi-Cue OCM for pilot-vehicle analysis of data obtained in an experimental study of simulated helicopter hover.[8] The goal was to demonstrate that the model could be used to analyze or predict the effects of simulator changes in a complex flight control task. Thus, to a degree, the investigation complements the earlier studies which were either completely analytic or involved data from relatively simple control tasks. It is worth mentioning that this study is of broader interest than the simulation context because of the opportunity to compare model results with data in what appears to be, in certain ways, the most complex steady-state control task modelled by the OCM (or any other pilot model).

Section II of the report describes the general multi-cue OCM used for the analysis. In section III, the particulars of applying the model to the specific task being investigated are presented and model predictions are then compared with experimental data. The last section summarizes the results and presents conclusions.

---

5 Baron, S., A Multi-Cue OCM for Analysis of Simulator Configurations," BBN Report No. 4373, April 1980.

6 Op.Cit. (Baron, Muralidharan, Kleinman [1])

* Personal Communication with B.T. McKissick, NASA-LRC.

7 Op.Cit. (Baron [5])

8 Ricard, G.L, Parrish, R.V., Ashworth, B.R. and Wells, M.D., "The Effects of Various Fidelity Factors on Simulated Helicopter Hover," NAVTRAEQUIPCEN IH-321, January 1981.

SECTION II
A MULTI-CUE OPTIMAL CONTROL MODEL (OCM)

The OCM has been documented extensively (see Baron and Levison[9] for a review) so its discussion here will be brief, with emphasis on those aspects of the model that are of special relevance to simulator evaluation. First, we will give a general description of a simulation system in the next paragraph, to provide a background for the pilot model description given in the following paragraphs. The discussion is largely taken from a recent report[10] describing a version of the model that incorporates explicitly effects that are germane to simulator analysis.

GENERAL SYSTEM DESCRIPTION

A detailed block diagram of both the system and the OCM pilot model is given in Figure 1. The system portion (outside the dashed box) provides for representations of control stick dynamics, vehicle dynamics, and the dynamics associated with the simulator drive logic (e.g., a motion base washout filter) and its hardware (e.g., the servo drives). As shown, the two inputs to the system are the set of controls ($\underline{u}$) generated by the pilot, and the system disturbances ($\underline{d}$) which perturb the vehicle states. The set of system outputs is the cue set provided by the simulator to the pilot's various sensory systems. The OCM system modelling approach involves: (1) a linearization of the relevant dynamics associated with each of the subsystems; and (2) the construction of a state-variable representation of the combined system dynamics. The resulting vector-matrix state equation has the following form:

$$\underline{\dot{x}}(t) = \underline{A}\underline{x}(t) + \underline{B}\underline{u}(t) + \underline{E}\underline{w}(t) \qquad (2.1)$$

where $\underline{x}(t)$ is a vector whose components are the states of the simulator system, $\underline{u}(t)$ a vector of pilot control inputs, and $\underline{w}(t)$ a vector of white driving noise processes, the latter included to model the system disturbances. In general, the matrices $\underline{A}$, $\underline{B}$, and $\underline{E}$ may all be time-varying (piece-wise constant) to reflect changes due to differing flight conditions. Moreover, the continuous matrices may include effects introduced by a digital solution of the system equations.[11]

The above system model includes all of the dynamics associated with all of the subsystems comprising the simulator.

---

[9] Baron, S., and Levison, W.H., "The Optimal Control Model: Status and Future Directions," Proceedings of the IEEE Conference on Cybernetics and Society, Boston, MA, Oct. 1980.

[10] Op. Cit. (Baron [5])

[11] Op. Cit. (Baron, Muralidharan, Kleinmann [1])

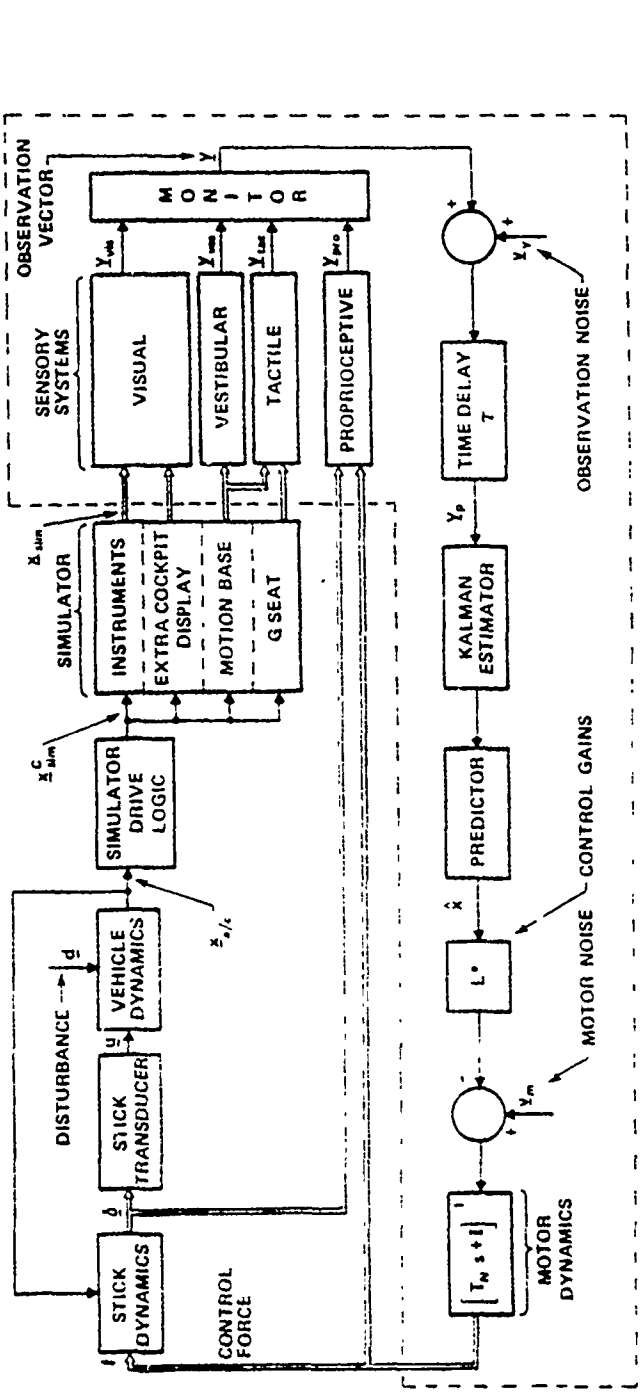

Figure 1. Pilot/Simulator Model

In general, it will also include dynamics associated with three other aspects of the closed-loop control task: (1) the disturbance or command model; (2) the dynamics which characterize the pilot's sensory capabilities; and (3) any dynamics which might be used to approximate other system characteristics which cannot be expressed directly in terms of linear first-order vector-matrix equations. We discuss these points in the following paragraphs.

Insofar as disturbance or command inputs can be represented by rational noise spectra (for example, gust disturbances may be so modelled), they can be incorporated in the system model by first determining the appropriate shaping filter, which, when acting on white noise, generates the desired input spectrum. By expressing this shaping filter in state-variable format, the system (2.1) may then be augmented to generate appropriate input states which are driven by the white noise process vector $\underline{w}(t)$, through the disturbance input matrix $\underline{E}$.

If the pilot's sensory dynamics are deemed relevant to understanding closed-loop performance in the given task, the dynamics may be expressed in state variable form, and used to augment the system dynamics of (2.1). We will discuss this at greater length in the next section, in our description of the pilot portion of the closed-loop system.

System dynamics which, after linearization, are not directly expressible in the form of (2.1) may be included in the system description by first finding a suitable state-variable approximation and then augmenting (2.1) with this approximation. In particular, delays associated with simulator cueing, are conveniently handled by this approach. An appropriate Pade filter approximation is found, and the associated state variable dynamics are used to augment the system dynamics of (2.1).*

In summary, the system (2.1) not only includes the explicit dynamics of the various simulator subsystems, but also the implicit dynamics associated with the disturbance spectra, the relevant sensory dynamics of the pilot, and any additional approximations deemed necessary for accurate system modelling.

The inclusion of these various elements in the system model is significant because they will then be automatically reflected in the "internal model" of the pilot as represented in the OCM. This is tantamount to assuming that the trained pilot will compensate for predictable correlations in the disturbance inputs and for his own sensory limitations, as well as for the particular system being controlled.

---

* Note that this is distinct from the basic human time delay that is assumed to be the same for all information channels and is included as a pure transport lag in the pilot model. Pade approximations are used to account for different incremental delays in various cue generation paths.

OVERVIEW OF THE PILOT MODEL

The basic assumption underlying the optimal control model for the pilot is that the well-trained, well-motivated human controller will act in a near optimal manner subject to certain internal constraints that limit the range of his behavior and also subject to the extent to which he understands the objectives of the task. When this assumption is incorporated in the optimal control framework and when appropriate limitations on the human are imposed, the structure shown within the dashed lines of Figure 1 results. In discussing this structure it is convenient and meaningful to view this model as being comprised of the following: (1) a display interface which converts system state variables and pilot control outputs into a set of "displayed" variables $\underline{y}(t)$; (2) an "equivalent" perceptual model that translates these variables into noisy, delayed "perceived" variables denoted by $\underline{y}_p(t)$; (3) an information processor, consisting of an optimal (Kalman) estimator and predictor that generates the minimum-variance estimate $\hat{\underline{x}}(t)$ of $\underline{x}(t)$; (4) a set of "optimal gains," $\underline{L}^*$, chosen to minimize a quadratic cost functional that expresses task requirements; and (5) an equivalent "motor" or output model that accounts for "bandwidth" limitations (frequently associated with neuromotor dynamics) of the human and his inability to generate noisefree controls or to know the control input exactly. We now discuss these model components in greater detail.

Display Interface

The display interface provides a means for transforming the system state variables and the pilot's control actions into a display "vector" which represents the set of all of the information available to the pilot. The components of the display vector are assumed to be linear combinations of the state and control variables, and are defined by the following m-dimensional vector equation:

$$\underline{y}(t) = \underline{C}\underline{x}(t) + \underline{D}\underline{u}(t) \tag{2.2}$$

where $\underline{C}$ and $\underline{D}$ may be time-varying (piece-wise constant) to account for changes in the quantities being displayed or "observed."

In the present context, we assume that the information available to the pilot is that which he obtains via his visual, vestibular, proprioceptive and tactile sensory systems. As shown in the figure then, the display vector $\underline{y}$ can be partitioned as follows:

$$\underline{y} = (\underline{y}_{VIS}, \underline{y}_{VES}, \underline{y}_{PROP}, \underline{y}_{TAC})^T \tag{2.3}$$

where $\underline{y}_{vis}$, $\underline{y}_{ves}$, $\underline{y}_{prop}$ and $\underline{y}_{TAC}$ are the outputs of the visual, vestibular, proprioceptive and tactile sensory systems. The individual display vectors associated with a particular modality

can include information provided by more than one cueing system which impinge on that same modality. Thus, for example, $\underline{y}_{vis}$ can include both out-the-window (visual) cues and additionally, available instrument (visual) cues.

In general, the processing provided by the pilot's sensory systems requires a model which involves not only a linear transformation of the system state (as in (2.2)), but also a dynamic transformation which accounts for any important dynamics of sensory processing (e.g., vestibular dynamics). As we noted earlier, this latter modelling requirement is implemented by assigning the sensory dynamics to the set of overall system dynamics, and appropriately augmenting the state equation of (2.1).[12]

Information Processing Limitations

Limitations on the pilot's ability to process information "displayed" to him are accounted for in the "equivalent" perceptual model. This model translates the displayed variables $\underline{y}$ into delayed, "noisy" perceived variables $\underline{y}_p$ via the relation

$$\underline{y}_p(t) = \underline{y}(t-\tau) + \underline{v}_y(t-\tau) \qquad (2.4)$$

where τ is an "equivalent" perceptual delay and $\underline{v}_y$ is an "equivalent" observation noise vector.*

The various internal time delays associated with visual, vestibular, central processing and neuro-motor pathways are combined and conveniently represented by this lumped equivalent perceptual time delay τ. Typical values for this delay are 0.2 $\pm$ .05 sec.[13]

Observation noise, $\underline{v}_y$, is included to account for the pilot's inherent randomness due to random perturbations in human response characteristics, errors in observing displayed variables, and attention-sharing effects which limit the pilot's ability to process accurately all the cues simultaneously available. In combination with the model of motor noise (described later), the model of observation noise provides a convenient and accurate means of modelling remnant and thus accounting for random control actions.

---

12 Op. Cit. (Baron, Lancraft, Zacharias [4]).

* The use of the word equivalent in this context is to emphasize that the parameters may be lumped representations of a variety of limitations that can not be "identified" separately by existing measurement techniques.

13 Kleinman, D.L., Baron, S., and Levison, W.H., "An Optimal Control Model of Human Response, Part I: Theory and Validation," Automatica, Vol. 6, pp. 357-369, 1970.

For manual control situations in which the displayed signal is large enough to negate the effects of limitations due to visual resolution thresholding, the autocovariance of each observation noise component appears to vary proportionally with mean-squared signal level. In such situations, the autocovariance may be represented as

$$V_i(t) = \pi P_i \sigma^2_{y_i}(t) \tag{2.5}$$

where $\sigma_{y_i}^2$ is the variance of the i^{th} output, P_i is the "noise/signal ratio" for the i^{th} display variable, and has units of normalized power per rad/sec. Numerical values for P_i of 0.01 (i.e., -20 dB) have been found to be typical of laboratory tasks involving the control of a single variable.[14]

The perceptual model defined by (2.4) and (2.5) applies to "ideal" display conditions, in which the signal levels are large with respect to both system-imposed and pilot-associated thresholds. To account for threshold effects we let the autocovariance for each observation noise process be

$$V_i(t) = P_i\left(\frac{\sigma_i^2}{K_i^2(\sigma_i, a_i)}\right) \tag{2.6}$$

where the subscript i refers to the i^{th} display variable. The quantity, $K(\sigma_i, a_i)$ is the describing function gain associated with a threshold device

$$K(\sigma, a) = \frac{2}{\sqrt{\pi}} \int_{\frac{-a}{\sigma\sqrt{2}}}^{\infty} e^{-x^2}\, dx \tag{2.7}$$

where "a" is the threshold and σ is the standard deviation of the "input" to the threshold device. The net result of this type of describing function model is to increase the observation noise covariance as the display signal variance becomes smaller relative to the threshold. The approach is similar to the statistical thresholds of signal detection theory.[15]

The sources of these threshold effects depend on the particular task being modelled. They may be associated with the system display implementation, for example, due to resolution limitations on a display screen; or, they may be associated with the pilot's sensory limitations, such as one might identify with visual acuity or motion-sensing thresholds.

One additional factor which tends to increase the observation noise (associated with any given display variable) is the pilot's attention-sharing limitations. Because the numerical value associated with the pilot's noise/signal ratio (P) has been found to be relatively invariant with respect to system dynamics

---

14 Ibid.

15 Green, D.M. and Swets, J.A., "Signal Theory and Psychophysics," New York, J. Wiley and Sons, 1966.

and display characteristics, we associate this parameter with limitations of the pilot's overall information-processing capability. This forms the basis for a model for pilot attention-sharing where the amount of attention paid to a particular display is reflected in the noise/signal ratio associated with information obtained from that display.[16] Specifically, the effects of attention-sharing are represented as

$$P_i = P_o / f_i \tag{2.8}$$

where P_i is the noise/signal associated with the i^{th} display. When attention is shared among two or more displays, f_i is the fraction of attention allocated to the i^{th} display, and P_o is the noise/signal ratio associated with full attention to the task.

The "monitor" block of Figure 1 is the mechanism for choosing attention levels. To find the fraction of attention f_i associated with the i^{th} display variable, we first assumed that the pilot need not share attention between modalities. Thus, if f^{VIS}, f^{VES}, f^{PROP} and f^{TAC} are the attention levels assigned to the individual modalities, we set each of the levels equal to unity:

$$f^{VIS} = f^{VES} = f^{PROP} = f^{TAC} = 1 \tag{2.9}$$

This assumption seems plausible but remains to be verified. Indeed, there is some evidence of attention-sharing between visual and motion cues, but it is not conclusive.[17]

Attention may have to be shared among the display variables within a particular sensory modality. This is certainly true for the visual modality and could possibly be the case for other modalities. There are two basic approaches to picking the attention levels; either they are computed to optimize performance or, more simply, they are picked by assumption. When the attentions are picked by assumption, it is most frequently assumed that the pilot devotes equal attention to each of the individual display variables; the attention fraction in that case is the reciprocal of the number of variables.

Estimation and Control Models

The optimal predictor, optimal estimator, and optimal gain matrix represent the set of "adjustments" or "adaptations" by

16 Levison, W.H., Elkind, J.I., and Ward, J.L., "Studies of Multivariable Manual Control Systems: A Model for Task Interference," NASA-Ames Research Center, NASA CR-1746, May 1971.

17 Levison, W.H. and Junker, A.M., "A Model for the Pilot's Use of Motion Cues in Steady-State Roll Axis Tracking Tasks," presented at AIAA Flight Simulation Technologies Conference, Arlington, TX, September 1978, AIAA Paper No. 78-1593.

which the pilot tries to optimize his behavior.* The general expressions for these model elements are determined by system dynamics and task objectives according to well-defined mathematical rules.[18] The controller is assumed to adopt a response strategy to minimize a weighted sum of averaged output and control variances as expressed in the cost functional:

$$J(\underline{u}) = E[\underline{y}^T(t)\underline{Q}_y\underline{y}(t)+\underline{u}^T(t)\underline{Q}_u\underline{u}(t)+\dot{\underline{u}}^T(t)\underline{R}_u\dot{\underline{u}}(t)] \qquad (2.10)$$

where $J(\underline{u})$ is conditioned on the perceived information $\underline{y}_p$.

The selection of the weightings $\underline{Q}_y$ = diag $[q_{y_i}]$, $\underline{Q}_u$ = diag $[q_{u_i}]$ and $\underline{R}$ = diag $[r_i]$ in $J(\underline{u})$ is a non-trivial step in applying the OCM. The most commonly used method for selecting reasonable a priori estimates for the output weightings is to associate them with allowable deviations in the system variables, and has been described in several recent applications of the OCM (see , for example, Levison and Baron).[19] The control related weightings may be chosen in a similar fashion or they may be picked up to yield a desired value of T_N, as discussed below. This method of choosing weightings has several advantages. Maximum or limiting values of system quantities are often easy to specify or elicit from pilots. In addition, with this normalization, the contribution of each term to the total cost depends on how close that quantity is to its maximum value; the penalty is relatively small when the variable is within limits but increases rapidly as the variable exceeds its limit.

The tandem of predictor and estimator generates a minimum variance estimate of the system state. As such, they (linearly) compensate for any time delays or noises introduced by the system and/or the operator. These elements incorporate "perfect" models of the simulation environment including models of the cue generation systems. ** Thus, the model predictions are appropriate for pilots who are well trained on the simulator.

Motor Model

Limitations on the pilot's ability to execute appropriate control actions and to have perfect knowledge of those actions

* The monitoring function, i.e. the selection of attentions, is also an adaptation mechanism when the attention fractions are chosen to optimize performance.

[18] Op. Cit. (Kleinman, Baron, Levison [13])

[19] Levison, W.H. and Baron, S., "Analytic and Experimental Evaluation of Display and Control Concepts for a Terminal Configured Vehicle," BBN Report No. 3720, July 1976.

** Indeed, they also include models of the pilot's own sensory limitations.

are accounted for in the motor model, which is composed of a white motor noise source and a first-order lag matrix. In the standard OCM, this model translates "commanded" controls, $\underline{u}_C$, into the output control actions $\underline{u}$ via the following relation:

$$\underline{T}_N\dot{\underline{u}} + \underline{u} = \underline{u}_C + \underline{v}_M \tag{2.11}$$

where $\underline{T}_N$ is an "equivalent" lag matrix and $\underline{v}_M$ is an "equivalent" motor-noise vector. The commanded control is given by

$$\underline{u}_C = \underline{L}^*\hat{\underline{x}} \tag{2.12}$$

where L^* are the optimal gains (that minimize $J(u)$) and $\hat{x}$ is the minimum variance estimate of $\underline{x}$ provided by the filter-predictor.

In laboratory tracking tasks with optimized control sticks, the motor lag parameters have been associated with the operator's neuro-motor time constant and values of T_N=.1 seconds are typical. The neuro-motor noise vector of (2.10) is provided to account for random errors in executing intended control movements, and, in addition, to account for the fact that the pilot may not have perfect knowledge of his own control activity. In the standard OCM, the motor noise is assumed to be a white noise, with autocovariance that scales with the control variance, i.e.,

$$V_{m_i}(t) = P_{m_i}\,\sigma_{u_i}^2(t) \tag{2.13}$$

where, typically, a value for P_m of .003 (i.e., a "motor noise ratio" of -25 dB) yields a good agreement with experimental results.

MODELS FOR CUE PERCEPTION

The previous section described the general characteristics and limitations associated with the perceptual portion of the optimal control model. Here, we provide a bit more detail concerning perceptual models for the sensory modalities considered most relevant to simulated flight control tasks as indicated in Figure 1.

Visual Perception Model

The most important input for simulation of flight control tasks is generally the visual input. The major simulator hardware is cockpit instrumentation and external visual field information. The modelling of the use of standard cockpit instruments has been the principal focus of OCM development and is relatively straightforward.

In contrast to the relatively well-defined set of visual cues provided by within-cockpit instrumentation, the extra-cockpit visual scene can provide the pilot with an exceptionally rich visual environment, even with a relatively

simple display. Attempting to describe and quantify this stimulus environment has been the object of many studies (e.g., Wewerinke).[20] The literature on scene attributes is extensive, but it is not clear that it is of much help in providing perceptual models for the analysis of closed-loop control. For this application, we must determine the cues available that are directly useful for controlling the aircraft. We must also determine the limitations imposed in using these cues in a manner that is consistent with the desired control system performance analysis. This implies determining observation noises, thresholds, etc. for the requisite information.

The analysis of a given scene to determine the particular cues available will, of course, depend on the scene. To model pilot processing of these cues one can take advantage of the "display vector" representation of the OCM (Equation 2.2) and the threshold capabilities of the model. Different approaches for accomplishing this have been suggested, but, for the most part, they all involve geometric analysis to determine the information available and the visual limitations (essentially, the effective perceptual thresholds) associated with that information.[21] Depending on the characteristics of the display, this type of geometric analysis of the scene may prove to be an entirely adequate approach to modelling the pilot's use of extra-cockpit visual cues. Thus, we would expect geometric analysis to suffice in the case of a perspective line drawing display. If, however, a more sophisticated display were utilized, which, perhaps, had surface shading and/or textural gradient capability, it may prove necessary to incorporate non-geometric models of visual cue processing in the optimal control model analysis.

It should be emphasized that these are essentially theoretical approaches to modelling the utilization of external visual cues in flight control tasks. Even though the data obtained thus far tend to support the utility of the approaches, they are of a very limited nature and much more is needed before one can consider the approaches as truly validated.

Vestibular Perception Model

Models of vestibular motion perception have been the subject of study for a number of years, and it is beyond the scope of this report to attempt to summarize this work. Instead, we refer the reader to a relatively recent review of motion cue models by

[20] Wewerinke, P.H., "A Theoretical and Experimental Analysis of the Outside World Perception Process," Proceedings of the Fourteenth Annual Conference on Manual Control, NASA Conf. Pub. 2060, Nov. 1978.

[21] Baron, S. and Levison, W.H., "Display Analysis with the Optimal Control Model of the Human Operator," Human Factors, Vol. 19, No. 5, pp. 437-457, Oct. 1977.

Zacharias,[22] in which a number of these models are described and critically reviewed.

Figure 2 shows a vestibular model in block diagram form. The upper portion models the semicircular canals as transducers of angular velocity, while the lower portion models the otoliths as transducers of specific force. This model includes both the dynamics associated with perception of motion cues and the resolution or threshold limitations.

In many situations, the signals being sensed by the vestibular system are within its bandpass. In such cases, it is possible to neglect vestibular dynamics and, thereby, reduce model and computational complexity. Then, one would simply incorporate the informational variables provided by motion in the display vector along with the appropriate threshold limitations.

Proprioceptive and Kinesthetic Models

For many simulator studies, but not for the one examined in this report, the inclusion of proprioceptive or kinesthetic cues available from a simulator control loading system are of concern. We are not considering proprioceptive cues for vehicle motion or orientation; the reader is referred to Borah, Young and Curry[23] for some preliminary considerations along these lines.

We note as a matter of general interest that the proprioceptive cues yield observations of stick-position and stick-rate and that the kinesthetic cue provides an observation of stick force. Including such observations in the display vector is straightforward but there are some problems. A major problem is that one must specify observation noises, thresholds and other limitations associated with these "control observations" and these are unknown at present. This is an area for further research.

G-Cuing Devices

The incorporation of cues from g-seats, helmet loaders, etc. into the OCM is handled in the same fashion as are other sensory cues. In particular, any significant hardware dynamics can be included as part of the system dynamics. Sensory dynamics, if important, are also added to the system dynamics, as discussed previously. The informational cues available from the devices are added to the display equation (2.2) and noises and other limitations in perceiving these variables must be determined.

---

22 Zacharias, G.L., "Motion Cue Models for Pilot-Vehicle Analysis," AMRL-TR-78-2, Wright-Patterson Air Force Base, Ohio, May 1978.

23 Borah, J., Young, L.R., and Curry, R.E., "Sensory Mechanism Modeling," AFHRL Tech Rept. AFHRL-TR-78-93, Air Force Human Resources Laboratory, Wright-Patterson AFB, Dayton, OH, Oct. 1977.

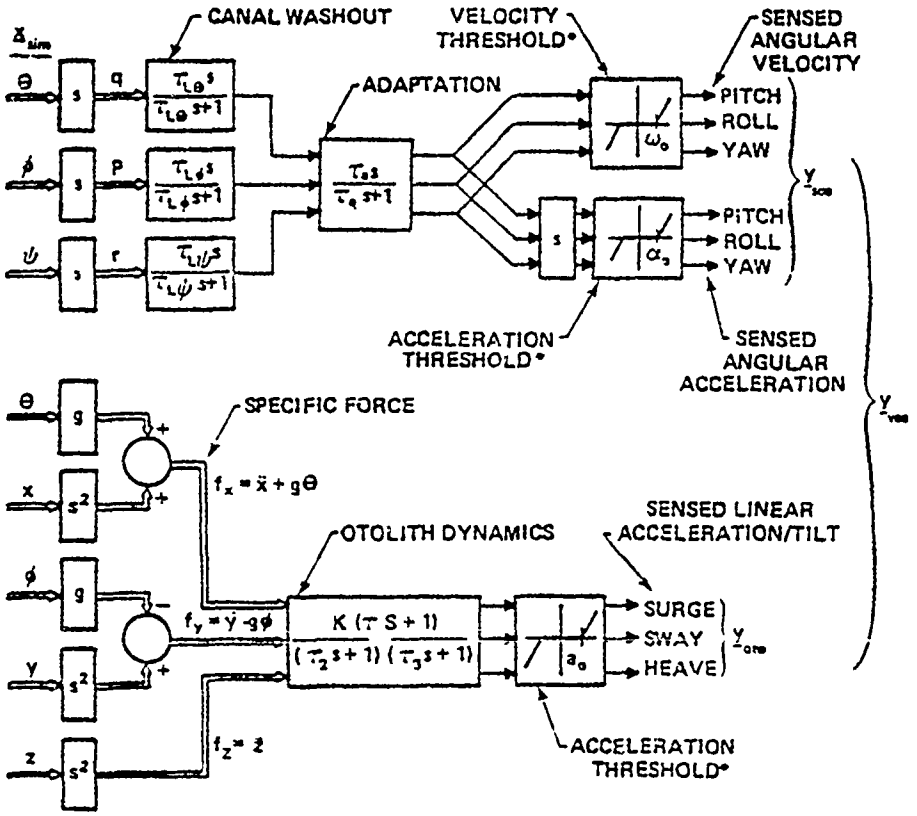

*THRESHOLD VALUES SPECIFIED INDIVIDUALLY FOR EACH AXIS

Figure 2. Vestibular Model

Unfortunately, none of the limitations associated with perceiving these cues is very well known quantitatively, at least in terms appropriate for the detailed control systems analyses for which the OCM is designed.

As has been done with other sensory cues, until better information becomes available, we will assume that the devices provide the appropriate state information directly and that the noise ratios associated with the perception of the variables are parameters that are initially set equal to those for visual inputs while thresholds are parameters. In addition, as indicated in equation (2.9), we will assume that attention-sharing between g-cues and cues provided by other modalities is not required.

SECTION III
APPLICATION OF OCM TO SIMULATED HOVER TASK

In this section, the task considered in the experimental simulation study is summarized briefly. (A more detailed review of this study is beyond the scope of this report but may be found in Ricard, et al.)[24] Then, the representation and specification of the task and pilot in the OCM framework are described. Finally, model predictions are presented and compared with the observed data.

GENERAL TASK DESCRIPTION

The experiment was designed to examine the effects on hover control of motion cues (as provided by a motion platform or g-seat) and of delays in the generation of visual cues. The simulated flight task corresponded to maintaining a Huey Cobra helicopter in a high hover relative to a ship moving at 15 knots. The desired hover position was fifty feet from the ship in line with a diagonal deck marking and at a mean height of twenty feet above the deck. The helicopter was subjected to turbulence modelled by Dryden gust spectra appropriate to an altitude of forty feet. Motions of the deck of the ship could also be simulated and the presence or absence of such ship motion was an experimental variable.

The data collected were rms values or tracking errors (rail-rail, bow-stern and height), helicopter pitch and roll and positions of controls (collective, pitch and roll cyclic, and rudder pedal).

MODEL SPECIFICATION

As indicated in section II, to analyze the task with the OCM, we must specify system dynamics, disturbances, displays (including cues), a performance objective and the assumed pilot limitations. Each of these is discussed below.

System Dynamics and Disturbances

A linearized set of equations of motion for the Huey Cobra, in state-variable format (Equation 2.1), was provided by Sperry Support Services, NASA-LRC.[25] These equations were obtained from the full nonlinear system simulation by means of a special program designed to develop such linear models.[26]

---

24 Op. Cit. (Ricard, et al. [8])

25 Carzoo, S. and Leath, B., "A Linearized Helicopter Model," Sperry Support Services, Report No. SP-710,018, Model 1980.

26 Dieudonne, J.E., "Description of a Computer Program and Numerical Techniques for Developing Linear Perturbation Models from Nonlinear Simulations," NASA TM 78710, July 1978.

Because of the 15 knot sideslip, decoupling of lateral and longitudinal helicopter motions did not appear to be justified (this was later verified). In addition, it did not seem appropriate to ignore the helicopter rotor dynamics. Thus, the basic equations of motion involved seventeen state variables: three positions (relative to the deck) and three linear velocities (in body axes); three body angular rates and attitude angles; and five states describing the rotor dynamics. Twelve additional state variables were required to model the stability augmentation system (SAS) of the helicopter. The state equations used in this analysis are given in Appendix A.

Dryden gust spectra were used to model the turbulence environment. In particular, the vehicle body axis gust disturbances u_g, v_g and w_g, were generated by passing white noise through filters so as to yield gust spectra appropriate to the forty foot altitude and fifteen knot airspeed of the helicopter. The rms intensity levels of the gusts u_g,v_g and w_g were 5 ft/sec, 5 ft/sec and 1.42 ft/sec, respectively. The state-variable models for the gusts are given in the appendix; five state variables are needed to model the three gusts.

In the experimental study, ship motion in each of the pitch, roll and heave axes was modelled by the sum of four sine waves. These inputs drove g-seat bladders upon which the ship model was mounted. It is theoretically possible to duplicate these inputs exactly but this would require twelve more state variables. Furthermore, it would be necessary to conduct a very careful analysis of the amplitudes of the motion as seen through the visual display system in order to model the effects of this ship motion precisely. For this analysis a much simpler approach was used. Only heave of the deck was considered and this was modelled by passing white noise through a second order filter; the parameters of this filter were selected so that the autocorrelation of this input matched that of the heave motion input used in the simulation. The rms level of the input used for this study was set at 3.5 feet, corresponding to the five foot *maximum* heave of the landing pad reported by Ricard et al.[27]

In the OCM analysis, ship movement was treated as a "display" disturbance; i.e., it was added to the pilot's perception of vertical error relative to the landing pad. The pilot's assumed objective was to maintain the helicopter's position relative to the mean position of the deck.

When the coupled vehicle dynamics, the rotor dynamics, the SAS and the gust and ship motion disturbances are all included, there are 36 state variables needed to model the "system" and environment (34 states for the case of no ship motion). Moreover, this does not even include any state variables to account for simulator dynamics or human sensory dynamics. This

27 Op. Cit. (Ricard et al. [8])

is, to our knowledge, a significantly larger problem than any previously treated with the OCM and, indeed, required modification of existing analysis programs to accommodate.

Simulator and Perceptual Models

Detailed descriptions of the motion and visual systems employed in the helicopter simulation are described in Ricard, et al.[28] Because of the complexity of the basic problem, as noted above, and the limited scope of this effort, these systems will be approximated in the simplest fashion possible. In particular, we will assume that any dynamics associated with motion cueing or sensing can be neglected. We also assume that differential delays between motion and visual cues can be neglected. These two assumptions have been made to avoid the necessity of having to introduce additional state variables. The assumption concerning the dynamics associated with motion cueing and sensing has proven to be reasonable in several previous studies. The assumption concerning the differential delays is less tenable, particularly when additional delay is added to the visual channel. Nonetheless, as we will see later, these assumptions appear quite adequate with respect to capturing much of what is in the data.

Thus, we treat the cue generation and perception problem on an informational level; i.e., we determine what control related information is available from the various cues and the corresponding perceptual limitations (mainly delay and thresholds).

The total delays for the various cues reported by Ricard, et al.[29] (including sampling and computational delays) are 77 ms for the VMS motion platform, 82 ms for the g-seat and 62-69 ms for the visual display.* We will assume an "average" delay of 70 ms for all cues.

The visual display provided a view of the ship, the horizon and a dimly lit Head-Up Display (HUD) to provide position reference information, otherwise denied by a limited field of view (48^{o} by 26^{o}). The TV display had a resolution of 9 minutes of arc ($.15^{o}$). It was assumed that from this external view display, the pilot could obtain both position information (relative to the landing pad) and attitude information. As is normally the case in applying the OCM, it was also assumed that rates of change of these variables could also be perceived.

---

[28] Ibid

[29] Op. Cit. (Ricard, et al. [8])

* The visual delays were different for translation (62 ms) and rotation (69 ms).

Visual thresholds for the various variables were computed using the method described in Baron, Lancraft and Zacharias.[30] These calculations are based on an analysis of the potential cues and depend on the geometry of the situation and on the discrimination and/or resolution capabilities of the human controller and of his equipment. In this case, the resolution limit of the display (.15°) is greater than that determined for human trackers in previous studies (.05°), so that it is used in resolution-determined thresholds. The geometric factors of importance are field of view and distance from and above the object being used to obtain the cue. The values of the visual thresholds determined from this analysis are given in Table 1.

The motion platform was assumed to provide the pilot with linear accelerations (a_x, a_y, a_z) and body angular rates and accelerations (p,q,r and $\dot{p},\dot{q},\dot{r}$). Thresholds for perception of these variables were based on the values given in Baron, Lancraft and Zacharias[31] and are listed in Table 1.

The g-seat was assumed to provide the pilot with surge acceleration and with pitch and roll rates and accelerations.* Perceptual thresholds for this type of cueing have not been measured, but it was felt that the g-seat did not provide cues as faithfully as the motion platform. Therefore, thresholds for g-seat cues were arbitrarily set to be 20 per cent higher than for the corresponding thresholds for platform motion indicated in Table 1.

Performance Criteria

As discussed in Section II, application of the OCM requires specification of a quadratic cost function. This involves specifying the variables to be considered and the weightings associated with those variables. The weightings can be associated with allowable deviations or with human subjective criteria or limitations. Here, because there was no opportunity to discuss performance objectives with the pilots, we made somewhat arbitrary initial assumptions concerning allowable deviations and then adjusted them via a brief preliminary sensitivity analysis to obtain reasonable agreement with the data for the fixed base, no added delay, no ship motion condition. The weights were then fixed for the rest of the analysis. The output and control variables included in the cost functional along with the corresponding deviations and weightings resulting from the preliminary analysis are listed in Table 2. Though not shown in Table 2, the cost functional also included control rate terms whose weightings were chosen to yield a "neuromotor" response lag of T_N = .1 second in each control channel.

30 Op Cit. (Baron, Lancraft, Zacharias [4])

31 Op. Cit. (Baron, Lancraft, Zacharias [4])

* Personal communication with Russell Parrish of NASA, LRC.

TABLE 1. PERCEPTUAL THRESHOLDS*

Variable	Visual	Motion Platform	G-Seat
x, ft	1.68	--	--
$\dot{x}$, ft/sec	.72	--	--
y, ft	.07	--	--
$\dot{y}$, ft/sec	.30	--	--
z, ft	.74	--	--
$\dot{z}$, ft/sec	.34	--	--
a_x, ft/sec^2	--	.053	.0636
a_y, ft/sec^2	--	.053	--
a_z, ft/sec^2	--	.053	--
ϕ, deg	.15	--	--
$\dot{\phi}$(p), deg/sec	.6	2.5	3.0
$\dot{p}$, deg/sec^2	--	.41	.49
θ, deg	.15	--	--
$\dot{\theta}$(q), deg/sec	.6	3.6	4.3
$\dot{q}$, deg/sec^2	--	.67	.80
ψ, deg	.15	--	--
$\dot{\psi}$(r), deg/sec	.6	4.2	--
$\dot{r}$, deg/sec^2	--	.41	--

*An entry of -- means that it is assumed that no information on the variable is provided by the modality

TABLE 2. PERFORMANCE COST FUNCTION PARAMETERS

Variable	"Maximum" Allowable Deviation (M_i)	Cost Weighting $\frac{1}{M_i^2}$
Rail-Rail Error, x, ft	10	.01
Bow-Stern Error, y, ft.	10	.01
Heave Error, z, ft.	10	.01
Roll, ϕ, rad. (deg.)	.1(5.7)	100
Pitch, θ, rad. (deg.)	.1(5.7)	100
Yaw, ψ, rad. (deg.)	.0175(1)	3280
Collective XAOS, in.	1	1
Roll Cyclic, YCS, in.	1	1
Pitch Cyclic, XCS, in.	1	1
Rudder, XTR, in.	.1	100

Other Model Parameters

The remaining model parameters to be specified are the operator's time delay and observation and motor noise/signal ratios. We assume a basic pilot delay of .2 seconds and a motor noise/signal ratio of -25 dB; these values are typical of those obtained in basic tracking experiments and have been used in numerous other applications.

To specify the observation noise, we must choose a base value for noise/signal ratio, P_i, and an attention-sharing algorithm. We assume a value of P_i of .04 (i.e., -14 dB) for all information variables, regardless of source. This value is higher than that associated with simple laboratory tasks in which operators receive extensive feedback and motivation and train to asymptotic performance. We believe the higher noise ratio is probably more appropriate for the experimental conditions and problem complexity being analyzed here.

We assume no attention-sharing between modalities or within the motion and proprioceptive modalities. Within the visual modality, we assume that the pilot shares attention equally among the six basic informational variables (position errors and vehicle attitudes).*

MODEL-DATA COMPARISONS

In the experimental study of Ricard et al.,[32] twelve conditions were investigated for the main experimental variables of motion cueing, visual delay and ship movement. These conditions are enumerated in Table 3. Each condition was repeated five times by each of 12 pilots, so that there were 60 runs per condition. The means and standard deviations for position errors, pitch and roll angles and control inputs obtained from these 60 runs, by experimental condition, are given in Table 4. Also shown in the last column of Table 4 is the variability in the various measures that is attributable to pilot difference alone (expressed as a standard error and computed from the ANOVA data in appendix B of (Ricard, et al.[33]). Unfortunately, this measure cannot be separated by experimental conditions on the basis of the data presently available.

The reader is referred to Ricard, et al., the cited reference, for a detailed analysis of the data using univariate analysis of variance. The discussion here will be very

* As is normally the case in applying the OCM, it is assumed that no diversion of attention is required to obtain the rate of change of a quantity from the same indication or cue as the quantity itself.

[32] Op. Cit. (Ricard, et al. [8])

[33] Ibid.

TABLE 3. EXPERIMENTAL CONDITIONS

CONDITION NO.	SHIP MOTION	VISUAL DELAY	MOTION BASE	G-SEAT
1	OFF	OFF	OFF	OFF
2	"	"	ON	"
3	"	"	OFF	ON
4	"	ON	OFF	OFF
5	"	"	ON	"
6	"	"	OFF	ON
7	ON	OFF	OFF	OFF
8	"	"	ON	"
9	"	"	OFF	ON
10	"	ON	OFF	OFF
11	"	"	ON	"
12	"	"	OFF	ON

TABLE 4. EXPERIMENTAL RESULTS (MEAN ± S.D.)

CONDITION NO. [1]	1	2	3	4	5	6	7	8	9	10	11	12	Pilot Variability (S.E)[2]
Rail-Rail Error,x,ft	9.5±5.8	7.3±3.0	9.3±4.9	12.2±6.6	8.9±3.8	10.2±4.3	10.9±4.8	7.9±3.3	10.3±5.0	11.0±5.3	8.7±3.4	10.1±3.8	5.41
Bow-Stern Error,y,ft	9.8±5.3	8.3±3.7	9.5±4.6	12.4±5.6	10.1±4 2	10.9±5.1	12.0±5.7	8.4±3.5	10.7±5.1	10.9±4.4	9.8±3.8	10.8±4.1	5.52
Altitude Error,h,ft	4.3±1.9	3.9±1.7	4.1±1.5	5.1±1.9	4.2±1.6	4.6±1.3	4.3±1.4	3.8±1.2	5.0±2.2	5.0±1.9	4.4±1.9	4.9±1.7	2.05
Roll Angle ø, rad.	071±.023	.066±.012	.071±.016	.080±.019	.072±.019	.080±.018	.070±.013	.071±.016	.073±.014	.081±.022	.072±.017	.081±.020	.021
Pitch Angle,θ, rad	.083±.013	.083±.012	.082±.010	.085±.014	.08,±.009	.083±.009	.082±.010	.083±.012	.084±.012	.086±.012	.086±.011	.086±.013	.015
Collective XAOS,in.	.42±.21	.46±.25	.36±.14	.54±.36	.53±.35	.46±.20	.45±.19	.50±.28	.48±.24	.50±.38	.48±.28	.53±.29	.343
Roll Cyclic YCS,in.	.41±.13	.33±.12	.41±.16	.41±.13	.36±.14	.43±.14	.38±.12	.37±.15	.40±.13	.45±.15	.36±.12	.43±.17	.246
Pitch Cyclic XCS,in.	.44±.16	.45±.13	.48±.24	.46±.14	.47±.16	.50±.14	.41±.14	.49±.17	.47±.17	.51±.17	.49±.13	.50±.21	.276
Rudder ,in.	063±.019	.068±.019	062±.016	.073±.022	.071±.018	.070±.016	.069±.0.7	.067±.020	.070±.022	.069±.024	.075±.021	.073±.018	.020

1. Condition numbers refer to Table 3.

2. Standard Error attributable to pilot variability alone, independent of condition.

brief. Significant effects were found on at least some measures for all the experimental variables, including the replicate and pilot variables. Indeed, the pilot factor was the major source of variance among the experimental variables. Motion cueing and visual delay had significant effects on the error measures but ship movement did not. Visual delay tended to increase the values of all system variables (error, states and controls).* Platform motion had a significant effect on vehicle roll attitude but not on pitch. Cyclic pitch increased with platform motion while cyclic roll decreased. Most pilots used more control when the ship motion was active. In addition to the main effects, there were a number of significant interactions, several of them involving the pilot factor. For example, the effect of visual delay was more pronounced when there was no ship motion.

The OCM as specified above was used to predict the rms values for all the variables of interest in each of the twelve conditions. The results are given in Table 5. These results were obtained with a fixed set of pilot parameters--the only changes made in the model from condition-to-condition were those corresponding to changes in the simulation (e.g., presence or absence of platform motion, g-seat or ship motion). It should also be noted that when used in this fashion, the OCM is intended to be representative of the performance expected of a highly trained, highly motivated pilot who has been allowed to reach asymptotic performance on each condition before data are taken.

Comparison of Tables 4 and 5 shows that all measures predicted by the model are within one standard error of the means, where the standard error is the measure of pilot variability mentioned above. This implies that the model is as good a predictor of a pilot's performance across the conditions as another pilot selected randomly from the group. Given the complexity of the problem and the assumptions made, this is a substantial achievement.

The model predictions are also within one standard deviation of the mean (where the variation is across subjects and replications) for virtually all measures and all conditions. The exceptions to this are, in a few instances, altitude error, cyclic pitch and pitch angle. These exceptions are well within two standard deviations of the mean and most are only marginally more deviant than one standard deviation.

Almost all model predictions are somewhat lower than the corresponding mean values determined experimentally. This suggests that the predictions could be brought in even closer agreement with the measured means by slight increases in the delay or noise parameters of the model.

* Except for two pilots whose performance, surprisingly, improved with delay.

TABLE 5. MODEL PREDICTIONS FOR DIFFERENT EXPERIMENTAL CONFIGURATIONS

Condition No.[1]	1	2	3	4	5	6	7	8	9	10	11	12
Rail-Rail , ft	9.5	8.2	9.2	9.9	8.6	9.7	10.0	8.5	9.3	10.6	8.9	10.0
Bow-Stern , ft	7.0	5.8	6.9	7.4	6.1	7.2	7.5	6.0	7.0	7.9	6.3	7.5
Altitude , ft	3.1	2.1	2.8	3.2	2.2	2.9	6.5	5.2	5.8	6.5	5.2	5.9
Roll , rad	.069	.062	.067	.070	.063	.069	.072	.063	.069	.074	.064	.071
Pitch , rad	.073	.070	.073	.074	.071	.074	.074	.071	.073	.075	.072	.074
Collective , in	.27	.23	.26	.27	.23	.26	.30	.24	.27	.30	.24	.28
Roll Cyclic , in	.29	.24	.28	.30	.25	.29	.31	.25	.29	.32	.26	.30
Pitch Cyclic, in	.29	.24	.29	.31	.26	.30	.31	.26	.29	.33	.27	.31
Rudder , in	.057	.056	.057	.056	.056	.057	.058	.056	.057	.058	.056	.057

[1]See Table 3.

If we examine the model results as a function of the main experimental variables, additional interesting features emerge.

Effects of Motion Cues. Figure 3 shows the effect of motion cues on rail-to-rail error, averaged over ship motion conditions, for the two delay conditions. It can be seen that the g-seat cues provide some improvement in performance and platform motion cues result in still less error. Further, the effect of motion cues does not appear to be significantly different for the two delay values; i.e., there does not appear to be a delay-motion interaction. These effects of motion cues exactly parallel the trends contained in the data. (Figure 13 of Ricard et al.).[34] Reference to Table 5 indicates that the remaining error terms show the same trends.

The effect of motion cues on the attitude variables (ϕ and θ) are shown in Figure 4. For this figure, model results for each motion condition were averaged across the delay and ship motion variables. The g-cues have only a very slight effect on the attitude variables. Platform motion results in demonstrably lower rms attitude values, with the effect for roll being greater than that for pitch. Again, these effects closely parallel those in the data (See Ricard, et al.[35], Figure 15) where there was a significant effect of motion on roll, but not on the pitch rms score.

The model does less well in predicting the effects of motion cues on control inputs, particularly pitch cyclic. As can be seen from Table 5, rms control inputs show very little differences between fixed base and g-seat condition, with, if anything, somewhat less activity with the g-seat on. However, control inputs are significantly reduced in the moving base condition. These trends reproduce those for the roll cyclic data. The collective and rudder data show virtually no difference between the fixed base and g-seat conditions, as is true for the model; however, while there appears to be no consistent effect of platform motion, Ricard reports that most pilots use significantly more collective and rudder for this condition, contrary to the predictions of the model. Finally, the model's trend for pitch cyclic does not agree at all with the observed data. In the experiment, pitch cyclic activity increases when motion cues are added and is greatest for the g-seat condition.

Visual Delay. The OCM predicts that all measurements, errors, states and controls will increase with the addition of delay. This pattern is also evident in the data. However, the increases predicted by the model tend to underestimate those observed in the data; i.e., the OCM is doing a better job of compensating for the delay than are the pilots. Also, while the model accurately predicts no motion-delay interaction, Figure 5

[34] Op. Cit. (Ricard et al. [8])

[35] Ibid.

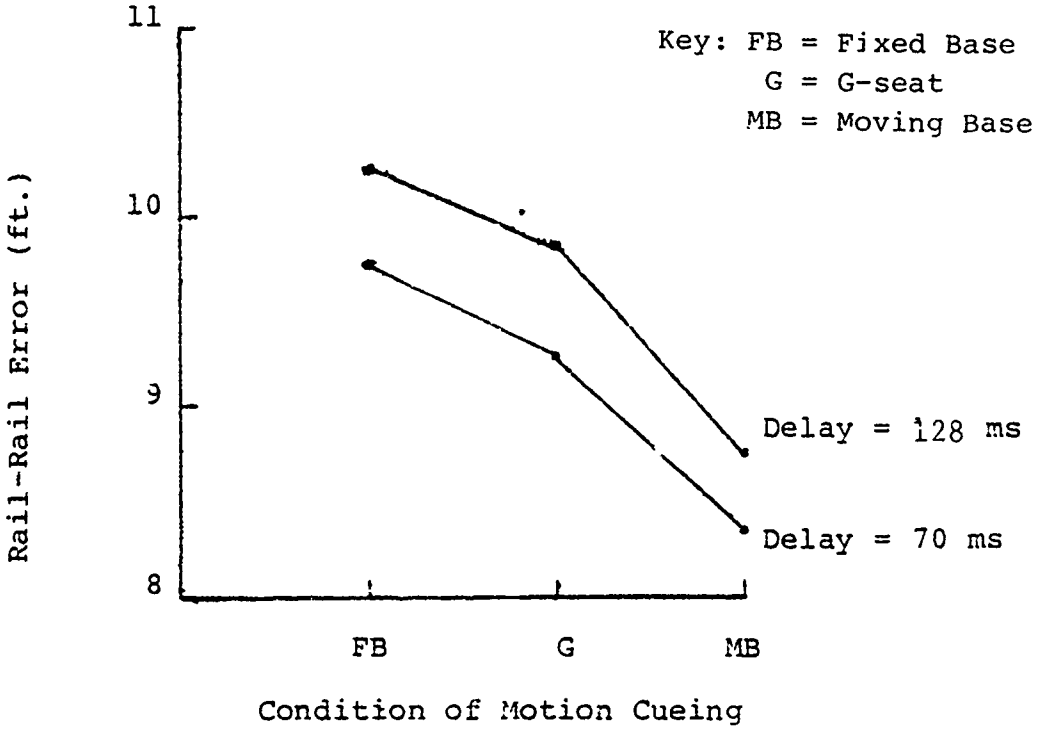

Figure 3. Effects of Motion Cues on Rail-Rail Hover Error.

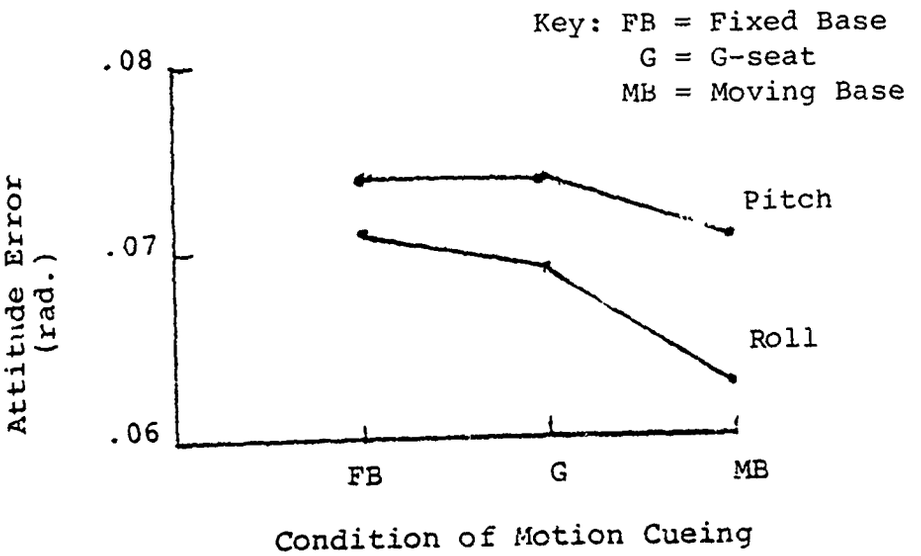

Figure 4. Effects of Motion Cues on Attitute Errors.

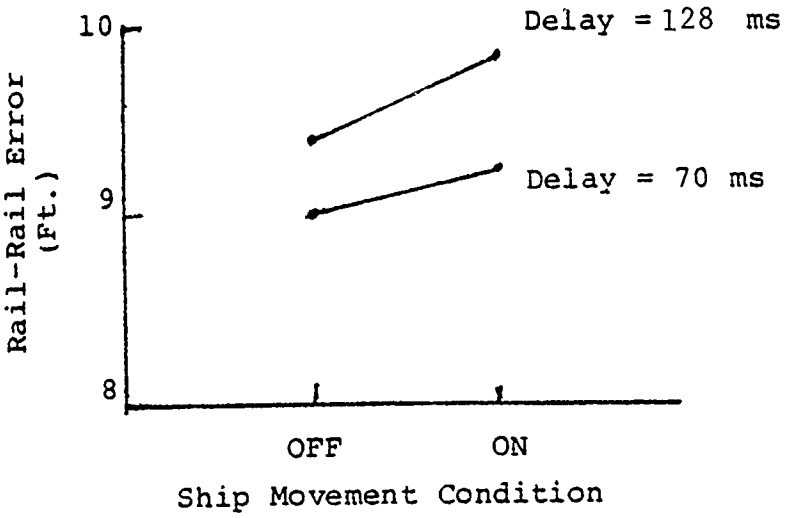

Figure 5. Effect of Ship Movement on Predicted Rail-Rail Hover Error

shows that the model does not predict the delay-ship motion interaction that was observed (Ricard et al., Figure 12).[36]

Ship Movement. The model predicts an increase in errors, attitude variables and control inputs when ship movement is present. The model results are not surprising from an analytic standpoint, but they are not entirely borne out by the data. For example, heave error increases with ship movement predicted by the model are much greater than those observed empirically. In addition, the model predicts increases in error regardless of the delay condition whereas the data show decreased errors with ship movement for the longer visual delay. Model trends are confirmed for the attitude variables, with ship movement increasing rms pitch and roll (for most pilots). Although the mean rms values of control variables do not exhibit consistent trends (Table 4), Ricard[37] does report a higher rudder activity, that is significant, with ship motion and that other control activity measures were also higher for most pilots; these results are in keeping with the model's predictions.

36 Ibid.

37 Ibid.

SECTION IV
SUMMARY AND CONCLUSIONS

This report has described the results of a small effort to apply the OCM to analyze data obtained in an experiment aimed at exploring simulator fidelity factors. The experimental task was to maintain a high hover position relative to a moving ship. Twelve skilled pilots performed the task for each of twelve experimental conditions. The main experimental variables were motion cue presentation, visual delay and ship movement.

The simulated hover task was specified in terms needed to apply the OCM. The vehicle dynamics were of substantial complexity, so simplifying assumptions with respect to simulator and perceptual characteristics were made for practical reasons. The parameters of the model relating to human limitations were selected mostly on the basis of previous work, though cost functional weightings were adjusted to give a reasonable "match" to the base experimental condition.

In general, the model predictions agree with the data to a substantial degree, with most of the differences being within the range of experimental variability. There appears to be a general trend for the model to be less sensitive to configuration changes than the mean measures. Unfortunately, while the data treatment allows us to determine the significance of a difference in performance resulting from a configuration change, it does not tell us the magnitude of the inter-subject variability in this difference (a paired-difference treatment of the data would provide this information). Thus, we cannot determine whether or not the differences predicted by the model are within the pilot-to-pilot variation. Nonetheless, there are two assumptions that could readily explain a lesser degree of model sensitivity to configuration change: (1) that performance has asymptoted in each condition so that the "pilot" has fully adapted to the configuration; and (2) that the basic pilot limitations (i.e., the OCM model parameters) do not change significantly throughout the experiment. It is highly suspect that these assumptions can ever be strictly valid in a factorial experiment of this size, given practical constraints. On the other hand, for this very reason, the model results may be a better measure of the differences due to configuration changes alone than are the data.

The excellent agreement between model and data for the fixed base, no additional delay case suggests that the information the pilot was obtaining from the external scene was adequately accounted for. Although we did not show the results, we also obtained model results under the assumption of no visual thresholds; these results failed to match the data. Thus, it would appear that the method used here for estimating visual thresholds from analysis of the external scene, proposed by

Baron, Lancraft and Zacharias, [38] is reasonable.

The model does particularly well in predicting the effects of motion cues on position errors and attitude angles. This suggests that the simple informational treatment of motion cues employed here was adequate for this task. Furthermore, both sensory thresholds assumed for these cues and the assumption of no attention-sharing within the motion-sensing modalities appear reasonable in light of the model-data agreement. A major caveat to these conclusions is that the model did fail to predict the effect of motion on pitch cyclic control, a fact that we are unable to explain based on our limited analysis. It should also be noted that one is unlikely to be able to separate definitively the various sources of pilot observation noise (thresholds, base noise/signal ratio and attention sharing logic) without designing experiments expressly for this purpose (see, e.g., Levison). [39]

The main effects of visual delay were also predicted by the model as was the lack of motion-delay interaction. The model predicts less degradation with delay than is observed in the "mean" rms performance measures. It is not clear that the lower sensitivity of the OCM to increases of delay is attributable entirely to the assumptions mentioned above. There is the possibility that the reduced stability margins in the added delay case cause the pilots to adapt their strategies in response to an increased tendency for Pilot Induced Oscillation (PIO) and the model does not account for this change. Further analysis would be needed to resolve this question.

The model was less successful in predicting the effects of ship movement, in particular in over-estimating the effects on heave error and in missing the ship movement/delay interaction. On the basis of the present analysis, we cannot tell whether this is simply the result of our approximation to the ship movement input or it is due to some other inadequacy of the model.

In sum, these results demonstrate a significant capability for predicting closed-loop system performance, and the effects on it of simulator deficiencies, for even highly complex tasks. When viewed in light of other recent studies of a similar nature, the results clearly point to the conclusion that the OCM can be very useful for predicting and analyzing engineering requirements for simulators. This includes the potential for design and evaluation of algorithms (such as washout filters or delay compensators) to ameliorate hardware deficiencies.

Several areas for further research are suggested by this effort. A major source of variance in the simulator study was

---

[38] Op. Cit. (Baron, Lancraft, Zacharias [4])

[39] Levison, W.H., "The Effects of Display Gain and Signal Bandwidth on Human Controller Remnant," AMRL-TR-70-93, March 1971.

the pilot factor; there were significant differences between pilots, both quantitatively and qualitatively. The development and application of the OCM has stressed modelling the performance of an "average" well-trained, well-motivated pilot. This is highly appropriate strategy for many problems of system design and evaluation. However, there are obviously individual differences and these, too, are important, particularly if one attempts to address training and/or "screening" issues. It is of interest, therefore, to determine the extent to which variations of parameters of the OCM can account for individual differences among skilled pilots or among pilots in various stages of training. To accomplish this in any definitive fashion would require a substantial empirical study involving a large number of subjects and a supporting analytic study. A less ambitious effort that might provide a useful start and insight, would be to attempt to reproduce the pilot-to-pilot differences in the existing hover data by means of a systematic sensitivity analysis.

Although the model did quite well in predicting the effects of motion cues, there are still several issues to be addressed. One specific issue is the disparity between modelling results and data in the control activity seen in the moving base condition. More generally, we need a basic and systematic empirical study of g-seats to get at the limits of their utility. Interpreting such studies using the OCM, especially in terms of perceptual limitations, would be very useful.

Finally, with respect to any of the simulation devices or limits examined here, it is important to investigate their effects on skill acquisition (i.e., rate of learning) and on transfer of training, as well as on performance. It may well be that a simulator enhancement does not improve asymptotic performance but does reduce training time or, conversely, that it improves simulator performance but not training. We believe that the OCM could provide very useful insights and measurements of the progress of training, but it will require research to extend it so that it will be applicable to the problem of skill acquisition. [40]

---

40 Op. Cit. (Baron and Levison [9])

REFERENCES

Ashworth, B.R., McKissick, B.T., and Parrish, R.V., "The Effects of Simulation Fidelity on Air-to-Air Tracking," Proc. of the Fifteenth Annual Conference on Manual Control, AFFDL-TR-79-3134, WPAFB, Ohio, Nov. 1979.

Baron, S., "A Multi-Cue OCM for Analysis of Simulator Configurations," Bolt Beranek and Newman Inc., Report No. 4374, April 1980.

Baron, S., Lancraft, R., and Zacharias, G., "Pilot/Vehicle Model Analysis of Visual and Motion Cue Requirements in Flight Simulation," Bolt Beranek and Newman Inc., Report No. 4300. Jan. 1980.

Baron, S., and Levison, W.H., "The Optimal Control Model: Status and Future Directions," Proc. of the IEEE Conference on Cybernetics and Society, Boston, MA, Oct. 1980.

Baron, S., and Levison, W.H., "Display Analysis with the Optimal Control Model of the Human Operator," Human Factors, Vol. 19, No. 5, pp. 437-457, Oct. 1977.

Baron, S., and Muralidharan, R., "The Analysis of Some Flight Control Simulator Characteristics Using a Closed-Loop Pilot Vehicle Model," Bolt Beranek and Newman Inc., Report No. 4329.

Baron, S., Muralidharan, R., and Kleinman, D.L., "Closed-Loop Models for Analyzing Engineering Requirements for Simulators," NASA CR-2965, Feb. 1980.

Borah, J., Young, L.R., and Curry, R.E., "Sensory Mechanism Modeling," AFHRL Tech. Rept. AFHRL-TR-78-93, Air Force Human Resources Laboratory, Wright-Patterson AFB, Dayton, OH, Oct. 1977.

Carzoo, S., and Leath, B., "A Linearized Helicopter Model," Sperry Support Services, Report No. SP-710,018, Model 1980.

Dieudonne, J.E., "Description of a Computer Program and Numerical Techniques for Developing Linear Perturbation Models from Nonlinear Simulations," NASA TM 78710, July 1978.

Green, D.M., and Swets, J.A., "Signal Theory and Psychophysics," New York, J. Wiley and Sons, 1966.

Kleinman, D.L., Baron, S., and Levison, W.H., "An Optimal Control Model of Human Response, Part I: Theory and Validation," Automatica, Vol. 6, pp. 357-369, 1970.

Levison, W.H., "The Effects of Display Gain and Signal Bandwidth on Human Controller Remnant," AMRL-TR-70-93, March 1971.

Levison, W.H., Baron, S., "Analytic and Experimental Evaluation of Display and Control Concepts for a Terminal Configured Vehicle," Bolt Beranek and Newman Inc., Report No. 3720, July 1976.

Levison, W.H., Elkind, J.I., and Ward, J.L., "Studies of Multivariable Manual Control Systems: A Model for Task Interference," NASA-Ames Research Center, NASA CR-1746, May 1971.

Levison, W.H., and Junker, A.M., "A Model for the Pilot's Use of Motion Cues in Steady-State Roll Axis Tracking Tasks," presented at AIAA Flight Simulation Technologies Conference, Arlington, TX, Sept. 1978, AIAA Paper No. 78-1593.

Ricard, G.L., Parrish, R.V., Ashworth, B.R., and Well, M.D., "The Effects of Various Fidelity Factors on Simulated Helicopter Hover," NAVTRAEQUIPCEN 1H-321, Jan. 1981.

Wewerinke, P.H., "A Theoretical and Experimental Analysis of the Outside World Perception Process," Proc. of the Fourteenth Annual Conference on Manual Control, NASA Conf. Pub. 2060, Nov. 1980.

Zacharias, G.L., "Motion Cue Models for Pilot-Vehicle Analysis," AMRL-TR-78-2, Wright-Patterson Air Force Base, Ohio, May 1978.

APPENDIX A

SYSTEM DYNAMICS

The "system" dynamics for application of the Optimal Control Model are expressed in state variable format:

$$\dot{\underline{x}} = \underline{Ax} + \underline{Bu} + \underline{Ew} \qquad (1)$$
$$\underline{y} = \underline{Cx} + \underline{Du}$$

where x is the system state-vector, u the vector of pilot control inputs, w a white-noise disturbance-vector and y the vector of displayed outputs. These vectors are defined below.

STATE-VECTOR

x: $\{u_g, v^*_g, v_g, w^*_g, w_g, x, y, h, u, v, w, p, q, r, \psi, \theta, \phi, W_{IM}, Q_E, \Omega, A_{ISS}, B_{ISS}, z_1, z_2, \ldots, z_{12}\}$

where

u_g: gust velocity along x-body axis, ft./sec.
v^*_g: dummy variable
v_g: gust velocity along y-body axis, ft./sec.
w^*_g: dummy variable
w_g: gust velocity along z-body axis, ft./sec.
SM: heave ship movement, ft.
SM: rate of change of SM, ft./sec. x: rail-to-rail error, ft.
y: bow-to-stern error, ft.
h: altitude error, ft.
u: linear velocity along x-body axis, ft./sec.
v: linear velocity along y-body axis, ft./sec.
w: linear velocity along x body axis, ft./sec.
p: roll rate, rad./sec.
q: pitch rate, rad./sec.
r: yaw rate, rad./sec.
ψ: heading angle, rad.
θ: pitch angle, rad.
ϕ: roll angle, rad.
W_{IM}: main rotor mean inflow velocity, ft./sec.
Q_E: engine torque, pound-ft.
Ω: main rotor angular velocity, rad./sec.
AISS: main rotor longitudinal flap angle, rad.
BISS: main rotor lateral flap angle, rad.
z_1-z_4: SAS states (roll channel)
z_5-z_8: SAS states (pitch channel)
z_9-z_{12}: SAS states (yaw channel)

Control-Vector

u: {XAOS, YCS, XCS, XTR}

where

XAOS: cockpit collective stick input, in.
YCS: cockpit roll cyclic stick input, in.
XCS: cockpit pitch cyclic stick input, in.
XTR: cockpit tail rotor pedal input, in.

Display (Output) Vector

The display vector depends on the cue condition as follows:

Fixed Base:

y_{FB}: $x,\dot{x},y,\dot{y},h,\dot{h},\psi,\dot{\psi},\theta,\dot{\theta},\phi,\dot{\phi},$

Motion Base

y_{MB}: $\{y_{FB},a_x,a_y,a_z,p,\dot{p},q,\dot{q},r,\dot{r}\}$

G-Seat

y_G: $\{y_{FB},a_x,p,\dot{p},q,\dot{q}\}$

where a_x,a_y,a_z (ft./sec.) are linear accelerations along the x,y,z body axis, respectively and the remaining variables are defined above.

As noted in the text, the equations for the gust states were derived from the Dryden model spectra and the ship motion equations were an approximation to the "sum of sines" input used in the simulation. The remaining state equations were provided by NASA and are the linearized perturbation equations about the equilibrium condition corresponding to a 15 knot steady side slip. The system matrices, {A,B,C,D,E}, used in Equation 1 are given below for the fixed base condition with ship movement included.

HUEY.DYN

COUPLED DYNAMIC EQUATIONS OF MOTION FOR
SIMULATED HUEY COBRA HELIOCOPTER.
WITH SHIP MOTION
FOR 15 KNOT STEADY SIDESLIP FLIGHT CONDITION
INCLUDES DRYDEN GUST MODEL FOR 40' HOVER AT 15 KNOT SIDESLIP.
STATES:UG,VG*,VG,WG*,WG,SM,SMDOT,X,Y,H,U,V,W,P,Q,R,PSI,THETA,PHI
WIM,QE,OMEGA,A1SS,B1SS,Z1-Z12
OUTPUTS*X,U,Y,YDOT,H,HDOT,PHI,PHIDOT,THETA,THETADOT,PSI,PSIDOT
CONTROLS:XAOS,YCS,XCS,THTR

SYSTEM UNSTABLE

TOTAL NO. NOISE STATES = 7

A MATRIX:

-5.109E-02	0.	0.	0.	0.
0.	0.	0.	0.	0.
0.	0.	0.	0.	0.
0.	0.	0.	0.	0.
0.	0.	0.	0.	0.
0.	0.	0.	0.	0.
0.	0.	0.	0.	0.
0.				
0.	-5.109E-02	0.	0.	0.
0.	0.	0.	0.	0.
0.	0.	0.	0.	0.
0.	0.	0.	0.	0.
0.	0.	0.	0.	0.
0.	0.	0.	0.	0.
0.	0.	0.	0.	0.
0.				
0.	-2.159E-02	-5.109E-02	0.	0.
0.	0.	0.	0.	0.
0.	0.	0.	0.	0.
0.	0.	0.	0.	0.
0.	0.	0.	0.	0.
0.	0.	0.	0.	0.
0.	0.	0.	0.	0.
0.				
0.	0.	0.	-6.334E-01	0.
0.	0.	0.	0.	0.
0.	0.	0.	0.	0.
0.	0.	0.	0.	0.
0.	0.	0.	0.	0.
0.	0.	0.	0.	0.
0.	0.	0.	0.	0.
0.				

0.	0.	0.	-2.677E-01	-6.334E-01
0.	0.	0.	0.	0.
0.	0.	0.	0.	0.
0.	0.	0.	0.	0.
0.	0.	0.	0.	0.
0.	0.	0.	0.	0.
0.	0.	0.	0.	0.
0.				
0.	0.	0.	0.	0.
0.	1.000E+00	0.	0.	0.
0.	0.	0.	0.	0.
0.	0.	0.	0.	0.
0.	0.	0.	0.	0.
0.	0.	0.	0.	0.
0.	0.	0.	0.	0.
0.				
0.	0.	0.	0.	0.
-9.500E-01	-3.100E-01	0.	0.	0.
0.	0.	0.	0.	0.
0.	0.	0.	0.	0.
0.	0.	0.	0.	0.
0.	0.	0.	0.	0.
0.	0.	0.	0.	0.
0.				
0.	0.	0.	0.	0.
0.	0.	0.	0.	0.
-7.070E-01	7.070E-01	0.	0.	0.
0.	3.600E+01	-1.280E+00	-1.280E+00	0.
0.	0.	0.	0.	0.
0.	0.	0.	0.	0.
0.	0.	0.	0.	0.
0.				
0.	0.	0.	0.	0.
0.	0.	0.	0.	0.
7.070E-01	7.070E-01	0.	0.	0.
0.	0.	1.280E+00	-1.280E+00	0.
0.	0.	0.	0.	0.
0.	0.	0.	0.	0.
0.	0.	0.	0.	0.
0.				
0.	0.	0.	0.	0.
0.	0.	0.	0.	0.
0.	0.	-1.000E+00	0.	0.
0.	0.	1.800E+01	-1.790E+01	0.
0.	0.	0.	0.	0.
0.	0.	0.	0.	0.
0.	0.	0.	0.	0.
0.				

-1.585E-02	0.	3.358E-03	0.	-4.331E-02
0.	0.	0.	0.	0.
-1.585E-02	3.358E-03	-4.331E-02	6.698E-02	2.079E+00
1.790E+01	0.	-3.214E+01	0.	3.956E-02
-1.546E-08	-1.640E-01	-9.638E+00	6.114E+00	-9.258E-04
-7.816E-12	0.	-8.765E+00	-3.239E-05	0.
0.	1.374E+01	-3.262E-05	0.	0.
0.				
-7.140E-02	0.	-1.751E-01	0.	7.696E-02
0.	0.	0.	0.	0.
-7.140E-02	-1.751E-01	-1.896E-02	-2.095E+00	7.549E-02
-1.748E+01	0.	7.696E-02	3.211E+01	1.345E-02
-6.567E-09	-6.420E-02	6.472E+00	9.705E+00	-3.932E-04
-4.974E-12	0.	1.332E+01	-1.376E-05	0.
0.	9.758E+00	-1.386E-05	0.	0.
1.719E+01				
3.843E-03	0.	-1.618E-02	0.	-6.102E-01
0.	0.	0.	0.	0.
3.845E-03	-1.618E-02	-6.102E-01	-1.809E+01	1.766E+01
8.730E-06	0.	2.001E+00	-1.235E+00	6.000E-01
-2.506E-07	-2.623E+00	4.046E+00	-3.986E+00	-1.501E-02
-1.251E-10	0.	1.142E+01	-5.250E-04	0.
0.	1.150E+01	-5.287E-04	0.	0.
0.				
-5.315E-03	0.	-2.628E-02	0.	-1.258E-02
0.	0.	0.	0.	0.
-5.315E-03	-2.628E-02	-1.258E-02	-3.758E-01	6.200E-02
2.704E-01	0.	0.	0.	1.105E-02
-5.394E-09	-5.273E-02	5.316E+00	7.971E+00	-3.230E-04
-4.026E-12	0.	1.094E+01	-1.130E-05	0.
0.	8.015E+00	-1.138E-05	0.	0.
8.790E+00				
-3.431E-04	0.	-9.183E-04	0.	-5.570E-03
0.	0.	0.	0.	0.
-3.431E-04	-9.183E-04	-5.570E-03	-1.414E-02	-1.151E-01
9.105E-09	0.	0.	0.	3.201E-03
-2.614E-10	-2.351E-03	1.758E+00	-1.132E+00	-1.565E-05
0.	0.	1.691E+00	-5.475E-07	0.
0.	-2.299E+00	-5.514E-07	0.	0.
0.				
1.734E-04	0.	2.061E-02	0.	3.277E-04
0.	0.	0.	0.	0.
1.734E-04	2.061E-02	3.277E-04	3.927E-03	-1.043E-03
-4.420E-01	0.	0.	0.	-1.358E-04
9.839E-05	8.869E-04	-8.941E-02	-1.341E-01	5.433E-06
6.711E-14	0.	-1.840E-01	1.901E-07	0.
0.	-1.348E-01	1.914E-07	0.	0.
-1.263E+01				

0.	0.	0.	0.	0.
0.	0.	0.	0.	0.
0.	0.	0.	0.	3.852E-02
1.001E+00	0.	0.	0.	0.
0.	0.	0.	0.	0.
0.	0.	0.	0.	0.
0.	0.	0.	0.	0.
0.				
0.	0.	0.	0.	0.
0.	0.	0.	0.	0.
0.	0.	0.	0.	9.993E-01
-3.844E-02	0.	0.	0.	0.
0.	0.	0.	0.	0.
0.	0.	0.	0.	0.
0.	0.	0.	0.	0.
0.				
0.	0.	0.	0.	0.
0.	0.	0.	0.	0.
0.	0.	0.	1.000E+00	-2.395E-03
-6.226E-02	0.	0.	0.	0.
0.	0.	0.	0.	0.
0.	0.	0.	0.	0.
0.	0.	0.	0.	0.
0.				
-9.799E-01	0.	-9.262E-01	0.	3.295E+00
0.	0.	0.	0.	0.
-9.799E-01	-9.262E-01	3.295E+00	5.307E-01	5.139E-01
3.834E-05	0.	0.	0.	-6.295E+00
-1.101E-06	7.267E+00	-1.121E+01	1.104E+01	-6.391E-02
-4.945E-10	0.	-3.163E+01	-2.306E-03	0.
0.	-3.186E+01	-2.322E-03	0.	0.
0.				
9.197E+00	0.	2.677E+01	0.	-1.254E+02
0.	0.	0.	0.	0.
9.197E+00	2.677E+01	-1.254E+02	1.944E+03	9.015E+02
-2.345E-03	0.	0.	0.	1.297E+02
-9.999E-01	-9.958E+03	-5.140E+04	2.527E+04	4.030E+00
3.492E-08	0.	-2.983E+04	1.410E-01	0.
0.	-6.472E+04	1.420E-01	0.	0.
0.				
-3.261E-03	0.	-9.490E-03	0.	4.460E-02
0.	0.	0.	0.	0.
-3.261E-03	-9.494E-03	4.446E-02	-6.893E-01	-3.197E-01
8.314E-07	0.	0.	0.	-4.598E-02
3.546E-04	-2.023E-01	1.823E+01	-8.961E+00	-1.429E-03
-1.238E-11	0.	1.058E+01	-5.000E-05	0.
0.	2.295E+01	-5.035E-05	0.	0.
0.				

4.429E-03	0.	3.006E-03	0.	5.468E-04
0.	0.	0.	0.	0.
4.429E-03	3.006E-03	5.468E-04	3.147E-01	-1.000E+00
-9.109E-09	0.	0.	0.	7.158E-04
2.615E-10	-3.011E-03	-8.037E+00	-1.830E-02	1.566E-05
1.178E-12	0.	6.970E-03	5.478E-07	0.
0.	-1.068E+01	5.516E-07	0.	0.
0.				
2.987E-03	0.	-4.405E-03	0.	-4.367E-05
0.	0.	0.	0.	0.
2.987E-03	-4.405E-03	-4.367E-05	-9.997E-01	-3.146E-01
2.241E-08	0.	0.	0.	1.316E-03
-6.433E-10	4.627E-04	-2.269E-02	-8.011E+00	-3.852E-05
-1.620E-12	0.	1.067E+01	-1.348E-06	0.
0.	-1.731E-02	-1.357E-06	0.	0.
0.				
0.	0.	0.	0.	0.
0.	0.	0.	0.	0.
0.	0.	0.	0.	0.
0.	0.	0.	0.	0.
0.	0.	0.	0.	-2.500E+00
0.	0.	0.	0.	0.
0.	0.	0.	0.	0.
0.				
5.315E-04	0.	2.628E-03	0.	1.258E-03
0.	0.	0.	0.	0.
5.315E-04	2.628E-03	1.258E-03	-9.624E-01	-6.200E-03
-2.704E-02	0.	0.	0.	-1.105E-03
-8.554E-10	5.273E-03	-5.316E-01	-7.972E-01	1.500E+00
-2.000E+00	0.	-1.094E+00	-1.792E-06	0.
0.	-8.015E-01	-1.805E-06	0.	0.
-8.790E-01				
5.315E-04	0.	2.628E-03	0.	1.258E-03
0.	0.	0.	0.	0.
5.315E-04	2.628E-03	1.258E-03	-9.624E-01	-6.200E-03
-2.704E-02	0.	0.	0.	-1.105E-03
-8.554E-10	5.273E-03	-5.316E-01	-7.972E-01	1.500E+00
-2.000E+00	-4.000E-01	-1.094E+00	-1.792E-06	0.
0.	-8.015E-01	-1.805E-06	0.	0.
-8.790E-01				
0.	0.	0.	0.	0.
0.	0.	0.	0.	0.
0.	0.	0.	-1.250E+00	0.
0.	0.	0.	0.	0.
0.	0.	0.	0.	0.
0.	1.250E+01	-1.250E+01	0.	0.
0.	0.	0.	0.	0.
0.				

0.	0.	0.	0.	0.
0.	0.	0.	0.	0.
0.	0.	0.	0.	0.
0.	0.	0.	0.	0.
0.	0.	0.	0.	0.
0.	0.	0.	-2.500E+00	0.
0.	0.	0.	0.	0.
0.				
-7.205E-05	0.	-1.928E-04	0.	-1.170E-03
0.	0.	0.	0.	0.
-7.205E-05	-1.928E-04	-1.170E-03	-2.970E-03	9.758E-01
-3.032E-09	0.	0.	0.	6.723E-04
8.705E-11	-4.937E-04	3.692E-01	-2.378E-01	5.212E-06
2.608E-14	0.	3.552E-01	4.750E-01	-1.000E+00
0.	-4.828E-01	1.836E-07	0.	0.
0.				
-7.205E-05	0.	-1.928E-04	0.	-1.170E-03
0.	0.	0.	0.	0.
-7.205E-05	-1.928E-04	-1.170E-03	-2.970E-03	9.758E-01
-3.032E-09	0.	0.	0.	6.723E-04
8.705E-11	-4.947E-04	3.692E-01	-2.378E-01	5.212E-06
2.608E-14	0.	3.552E-01	4.750E-01	-1.000E+00
-4.000E-01	-4.828E-01	1.836E-07	0.	0.
0.				
0.	0.	0.	0.	0.
0.	0.	0.	0.	0.
0.	0.	0.	0.	2.625E+00
0.	0.	0.	0.	0.
0.	0.	0.	0.	0.
0.	0.	0.	0.	0.
1.250E+01	-1.250E+01	0.	0.	0.
0.				
0.	0.	0.	0.	0.
0.	0.	0.	0.	0.
0.	0.	0.	0.	0.
0.	0.	0.	0.	0.
0.	0.	0.	0.	0.
0.	0.	0.	0.	0.
0.	0.	-1.000E+01	0.	0.
0.				
2.550E-05	0.	3.031E-03	0.	4.820E-05
0.	0.	0.	0.	0.
2.550E-05	3.031E-03	4.820E-05	5.775E-04	-1.533E-04
4.420E-01	0.	0.	0.	-2.733E-05
1.447E-05	1.304E-04	-1.315E-02	-1.972E-02	-1.267E-06
-7.895E-15	0.	-2.705E-02	-4.432E-08	0.
0.	-1.982E-02	-1.338E+00	-7.042E-01	0.
-1.858E+00				

2.550E-05	0.	3.031E-03	0.	4.820E-05
0.	0.	0.	0.	0.
2.550E-05	3.031E-03	4.820E-05	5.775E-04	-1.533E-04
4.420E-01	0.	0.	0.	-2.733E-05
1.447E-05	1.304E-04	-1.315E-02	-1.972E-02	-1.267E-06
-7.895E-15	0.	-2.705E-02	-4.432E-08	0.
0.	-1.982E-02	-1.338E+00	-7.042E-01	-4.000E-01
-1.858E+00				
0.	0.	0.	0.	0.
0.	0.	0.	0.	0.
0.	0.	0.	0.	0.
7.250E+00	0.	0.	0.	0.
0.	0.	0.	0.	0.
0.	0.	0.	0.	0.
0.	0.	0.	0.	2.500E+01
-2.500E+01				

B MATRIX:

0.	0.	0.	0.
0.	0.	0.	0.
0.	0.	0.	0.
0.	0.	0.	0.
0.	0.	0.	0.
0.	0.	0.	0.
0.	0.	0.	0.
0.	0.	0.	0.
0.	0.	0.	0.
0.	0.	0.	0.
-2.757E-01	-2.831E-01	6.744E-01	-2.819E-06
-1.270E-01	4.302E-01	4.784E-01	1.500E+00
-4.459E+00	3.670E-01	5.617E-01	-4.569E-05
-1.043E-01	3.533E-01	3.929E-01	7.670E-01
-4.552E-03	5.460E-02	-1.129E-01	-4.765E-08
1.755E-03	-5.944E-03	-6.610E-03	-1.103E+00
0.	0.	0.	0.
0.	0.	0.	0.
0.	0.	0.	0.
1.235E+01	-1.014E+00	-1.556E+00	-2.007E-04
1.216E+03	-9.575E+02	-3.171E+03	1.227E-02
-4.311E-01	3.396E-01	1.124E+00	-4.352E-06
1.024E-02	2.235E-04	-5.239E-01	4.767E-08
-5.812E-03	3.446E-01	-8.443E-04	-1.173E-07
0.	4.036E-01	0.	0.
1.044E-02	4.539E-02	-3.92[illegible]E-02	-7.670E-02
1.044E-02	4.539E-02	-3.929E-02	-7.670E-02
0.	0.	0.	0.
0.	0.	3.678E-01	0.
-9.562E-04	1.147E-02	5.353E-02	1.587E-08
-9.563E-04	1.147E-02	5.353E-02	1.587E-08
0.	0.	0.	0.
0.	0.	0.	4.363E+00
2.582E-04	-8.739E-04	-9.719E-04	7.289E-01
2.582E-04	-8.739E-04	-9.719E-04	7.289E-01
0.	0.	0.	0.

E MATRIX:

1.598E+00	0.	0.	0.
0.	1.957E+00	0.	0.
0.	1.957E+00	0.	0.
0.	0.	1.957E+00	0.
0.	0.	1.957E+00	0.
0.	0.	0.	0.
0.	0.	0.	1.000E+00
0.	0.	0.	0.
0.	0.	0.	0.
0.	0.	0.	0.
0.	0.	0.	0.
0.	0.	0.	0.
0.	0.	0.	0.
0.	0.	0.	0.
0.	0.	0.	0.
0.	0.	0.	0.
0.	0.	0.	0.
0.	0.	0.	0.
0.	0.	0.	0.
0.	0.	0.	0.
0.	0.	0.	0.
0.	0.	0.	0.
0.	0.	0.	0.
0.	0.	0.	0.
0.	0.	0.	0.
0.	0.	0.	0.
0.	0.	0.	0.
0.	0.	0.	0.
0.	0.	0.	0.
0.	0.	0.	0.
0.	0.	0.	0.

C MATRIX:

0.	0.	0.	0.	0.
0.	0.	1.000E+00	0.	0.
0.	0.	0.	0.	0.
0.	0.	0.	0.	0.
0.	0.	0.	0.	0.
0.	0.	0.	0.	0.
0.	0.	0.	0.	0.
0.				
0.	0.	0.	0.	0.
0.	0.	0.	0.	0.
-7.070E-01	7.070E-01	0.	0.	0.
0.	3.600E+01	-1.280E+00	-1.280E+00	0.
0.	0.	0.	0.	0.
0.	0.	0.	0.	0.
0.	0.	0.	0.	0.
0.				

0.	0.	0.	0.	0.
0.	0.	0.	1.000E+00	0.
0.	0.	0.	0.	0.
0.	0.	0.	0.	0.
0.	0.	0.	0.	0.
0.	0.	0.	0.	0.
0.	0.	0.	0.	0.
0.				
0.	0.	0.	0.	0.
0.	0.	0.	0.	0.
7.070E-01	7.070E-01	0.	0.	0.
0.	0.	1.280E+00	-1.280E+00	0.
0.	0.	0.	0.	0.
0.	0.	0.	0.	0.
0.	0.	0.	0.	0.
0.				
0.	0.	0.	0.	0.
1.000E+00	0.	0.	0.	1.000E+00
0.	0.	0.	0.	0.
0.	0.	0.	0.	0.
0.	0.	0.	0.	0.
0.	0.	0.	0.	0.
0.	0.	0.	0.	0.
0.				
0.	0.	0.	0.	0.
0.	1.000E+00	0.	0.	0.
0.	0.	-1.000E+00	0.	0.
0.	0.	1.800E+01	-1.790E+01	0.
0.	0.	0.	0.	0.
0.	0.	0.	0.	0.
0.	0.	0.	0.	0.
0.				
0.	0.	0.	0.	0.
0.	0.	0.	0.	0.
0.	0.	0.	0.	0.
0.	0.	0.	1.000E+00	0.
0.	0.	0.	0.	0.
0.	0.	0.	0.	0.
0.	0.	0.	0.	0.
0.				
0.	0.	0.	0.	0.
0.	0.	0.	0.	0.
0.	0.	0.	1.000E+00	-2.395E-03
-6.225E-02	0.	0.	0.	0.
0.	0.	0.	0.	0.
0.	0.	0.	0.	0.
0.	0.	0.	0.	0.
0.				

0.	0.	0.	0.	0.
0.	0.	0.	0.	0.
0.	0.	0.	0.	0.
0.	0.	1.000E+00	0.	0.
0.	0.	0.	0.	0.
0.	0.	0.	0.	0.
0.	0.	0.	0.	0.
0.				
0.	0.	0.	0.	0.
0.	0.	0.	0.	0.
0.	0.	0.	0.	9.993E-01
-3.844E-02	0.	0.	0.	0.
0.	0.	0.	0.	0.
0.	0.	0.	0.	0.
0.	0.	0.	0.	0.
0.				
0.	0.	0.	0.	0.
0.	0.	0.	0.	0.
0.	0.	0.	0.	0.
0.	1.000E+00	0.	0.	0.
0.	0.	0.	0.	0.
0.	0.	0.	0.	0.
0.	0.	0.	0.	0.
0.				
0.	0.	0.	0.	0.
0.	0.	0.	0.	0.
0.	0.	0.	0.	3.850E-02
1.000E+00	0.	0.	0.	0.
0.	0.	0.	0.	0.
0.	0.	0.	0.	0.
0.	0.	0.	0.	0.
0.				

D MATRIX:

0.	0.	0.	0.
0.	0.	0.	0.
0.	0.	0.	0.
0.	0.	0.	0.
0.	0.	0.	0.
0.	0.	0.	0.
0.	0.	0.	0.
0.	0.	0.	0.
0.	0.	0.	0.
0.	0.	0.	0.
0.	0.	0.	0.
0.	0.	0.	0.

NAVTRAEQUIPCEN 80-C-0055-1

DISTRIBUTION LIST

Naval Training Equipment Center 100
Orlando, Florida 32813

Document Processing Division 12
Defense Documentation Center
Cameron Station
Alexandria, Virginia 22314

American Psychological Assn. 1
Psyc. INFO Document Control Unit
1200 Seventeenth Street, NW
Washington, D.C. 20036

The Van Evera Library 1
Human Resources Research Organization
300 N. Washington Street
Alexandria, Virginia 22314

U.S. Coast Guard (G-P-1/62) 1
400 Seventh Street, SW
Washington, D.C. 20590

AFOSR/NL (Dr. A. R. Fregley) 1
Bolling AFB
Washington, D.C. 20332

Commander 3
HQ, TRADOC
Attn: ATTNG-PA
Ft. Monroe, Virginia 23651

PERI-OU 1
U.S. Army Research Institute for the
Behavioral & Social Sciences
5001 Eisenhower Avenue
Alexandria, Virginia 22333

AFHRL Technology Office 1
Attn: MAJ Duncan L. Dieterly
NASA-Ames Research Center
MS 239-2
Moffett Field, California 94035

Dr. Ralph R. Canter 1
U.S. Army Research Institute
Field Unit
P.O. Box 16117
Fort Harrison, Indiana 46216

Library 1
Division of Public Documents
Government Printing Office
Washington, D.C. 20402

JSAS Manuscript Office 3
1200 Seventeenth Street, NW
Washington, D.C. 20036

Human Factors Society 2
Attn: Bulletin Editor
P.O. Box 1369
Santa Monica, California 90406

Center Library 3
Naval Personnel Research and
Development Center
San Diego, California 92152

OASD (MRA&L)/Training 2
Room 3B922, Pentagon
Washington, D.C. 20301

Center for Naval Analyses 1
Attn: Dr. R. F. Lockman
2000 N. Beauregard Street
Alexandria, Virginia 22311

Director 2
Training Analysis & Evaluation Group
Department of the Navy
Orlando, Florida 32813

Personnel & Training Research 3
Programs
Office of Naval Research (Code 458)
Psychological Sciences Division
800 N. Quincy Street
Arlington, Virginia 22217

National Defense University 1
Research Directorate
Ft. McNair, D.C. 20319

Dr. D. G. Pearce 1
Behavioral Sciences Division
Defense and Civil Institute of
Environmental Medicine
P.O. Box 2000
Downsview, Ontario M3M, CANADA

Dr. Ralph Dusek 2
U.S. Army Research Institute for
the Behavioral and Social Sciences
5001 Eisenhower Avenue
Alexandria, Virginia 22333

Dr. J. Huddleston 1
Head of Personnel Psychology
Army Personnel Research Establishment
c/o RAE, Farnborough
Hants, ENGLAND

HumRRO/Western Division/Carmel Office
27857 Berwick Drive 1
Carmel, California 93923

National Aviation Facilities 1
Experimental Center
Library
Atlantic City, New Jersey 08405

Commanding Officer 1
Air Force Office of Scientific
Research
Technical Library
Washington, D.C. 20301

OUSDR&E (R&AT) (E&LS) 1
CDR Paul R. Chatelier
Room 3D129, The Pentagon
Washington, D.C. 20301

Chief of Naval Operations 1
OP-596
Washington, D.C. 20350

Chief of Naval Material 1
MAT 08D2
CP5, Room 678
Attn: Arnold I. Rubinstein
Washington, D.C. 20360

Office of Deputy Chief of Naval 1
Operations
Manpower, Personnel and Training
(OP-01)
Washington, D.C. 20350

Chief of Naval Operations 1
(OP-115/M. K. Malehorn)
Washington, D.C. 20350

Dr. Martin Tolcott 1
Office of Naval Research
800 N. Quincy Street
Department of the Navy
Arlington, Virginia 22217

Dr. Jesse Orlansky 1
Science and Technology Division
Institute for Defense Analysis
400 Army-Navy Drive
Arlington, Virginia 2-202

Technical Library 1
Naval Training Equipment Center
Orlando, Florida 32813

Dr. Donald W. Connolly 1
Federal Aviation Administration
FAA NAFEC ANA-230 Bldg 3
Atlantic City, New Jersey 08405

Technical Library 1
OUSDR&E
Room 30122
Washington, D.C. 20301

Commander 1
Naval Air Development Center
Attn: Technical Library
Warminster, Pennsylvania 18974

Assistant Secretary of the Navy 1
Research, Engineering & Systems
Washington, D.C. 20350

Chief of Naval Operations 1
OP-987H/Dr. R. G. Smith
Washington, D.C. 20350

Chief of Naval Operations 1
OP-593B
Washington, D.C. 20350

Commander 1
Naval Air Systems Command
Technical Library AIR-950D
Washington, D.C. 20361

Commander 2
Naval Air Systems Command
AIR 340F/CDR C. Hutchins
Washington, D.C. 20361

Naval Research Laboratory
Attn: Library
Washington, D.C. 20375 1

Headquarters Marine Corps
Code APC/LTC J. W. Biermas
Washington, D.C. 20380 1

Scientific Technical Information Office
NASA
Washington, D.C. 20546 1

Commander
Naval Air Test Center
CT 176
Patuxent River, Maryland 20670 1

Commanding Officer
Naval Education Training Program and Development Center
Attn: Technical Library
Pensacola, Florida 32509 1

Chief
ARI Field Unit
P.O. Box 476
Ft. Rucker, Alabama 36362 1

Chief of Naval Education and Training Liaison Office
AFHRL/OTLN
Williams AFB, Arizona 85224 6

Commander
Naval Weapons Center
Human Factors Branch
3194/R. A. Erickson
China Lake, California 93555 1

Commander
Naval Air Systems Command
AIR 4135B/LCDR J. H. Ashburn
Washington, D.C. 20361 1

Scientific Advisor
Headquarters U. S. Marine Corps
Washington, D.C. 20380 1

Chief of Naval Education and Training
Code 01A
Pensacola, Florida 32509 1

Federal Aviation Administration
Technical Library
Bureau of Research and Development
Washington, D.C. 20590 1

Dr. J. D. Fletcher
Defense Adv. Research Projects Agency (CTO)
1400 Wilson Boulevard
Arlington, Virginia 22209 1

Commanding Officer
Naval Aerospace Medical Research Laboratory
Department of Psychology (Code L5)
Pensacola, Florida 32512 1

Chief of Naval Air Training
Code N2
Naval Air Station
Corpus Christi, Texas 78419 1

Commander
Pacific Missile Test Center
Point Mugu, California 93042 1

Officer in Charge
Naval Aerospace Medical Research Laboratory
Attn: CDR Robert S. Kennedy
Box 29407
New Orleans, Louisiana 70189 1

Naval Aerospace Medical Research Laboratory
Code L-53/CAPT James Goodson
Pensacola, Florida 32512 1

Mr. Don Gum
AFHRL/OTT
Wright Patterson AFB, Ohio 45433 1

Mr. Thomas Longridge
AFHRL/OTR
Williams AFB, Arizona 85224 1

Mr. Brian Goldiez
PM TRADE
Attn: DRCPM-PND-RE
Naval Training Center
Orlando, Florida 32813 1

Dr. David C. Nagel 1
LM-239-3
NASA Ames Research Center
Moffett Field, California 94035

Mr. James L. Copeland 1
NASA Langley Research Center
MS 125-B
Hampton, Virginia 23365

David L. Key 1
Chief, Flight Control Division
USAARDC
Moffett Field, California 94035

Chief of Naval Operations 1
OP-501C/CDR Giles R. Norrington
Washington, D.C. 20350

Dr. Orvin Larson 1
Code P-306
NAVPERSRANDCEN
San Diego, California 92152

Mr. James Basinger 1
ASD/YWE
Wright Patterson AFB, Ohio 45433

Mr. Eric Monroe 1
AFHRL/OTR
Williams AFB, Arizona 85224

Dr. Kenneth Boff 1
AFAMRL/HEA
Wright Patterson AFB, Ohio 45433

Mr. Robert Wright 1
Aeromechanics Lab (USAAVRADCOM)
Ames Research Center, MS 239-2
Moffett Field, California 94035

Mr. Will Bickley 1
USARI Field Unit
P.O. Box 476
Ft. Rucker, Alabama 36362

AFHRL/TSZ 8
Brooks AFB, Texas 78235

Major Jack Thorpe 1
AFOSR/NL
Bolling AFB, D.C. 20332

Naval Air Development Center 1
Human Factors Engineering Division
Code 602/CDR Norman E. Lane
Warminster, Pennsylvania 18974